RESULTS AND DISCUSSION

3 RESULTS AND DISCUSSION

3.1 Design and synthesis of selective PPARα agonists

As a part of the on-going research in the field of PPARs to develop novel therapeutic agents for the treatment of metabolic disorders.[225,234-236] Several PPAR agonists were reported, which were developed by chemical modifications either in the lipophilic tail part or / and the central spacer region (linker) to modulate agonistic activity and subtypes selectivity.[45,235,237] It was also believed that chemical modification on the lipophilic and central spacer of PPARα/γ dual agonist may lead to safe and efficacious selective PPARα agonists. In this context it was intended to syntesize the compounds with potent PPARα selectivity with the desired efficacy and safety profile.

3.1.1 Oxime containing benzyl 1,3-dioxane-*r*-2-carboxylic acid derivatives as selective PPARα agonist

In the present series, the objective was to develop oxime containing benzyl 1,3-dioxane-*r*-2-carboxylic acid derivatives as highly potent and selective PPARα agonist, which was designed by bioisosteric replacement of rigid oxazole ring of the previously reported PPARα/γ dual agonist (**I**)[225] with a flexible lipophilic tail (**Figure 20**).

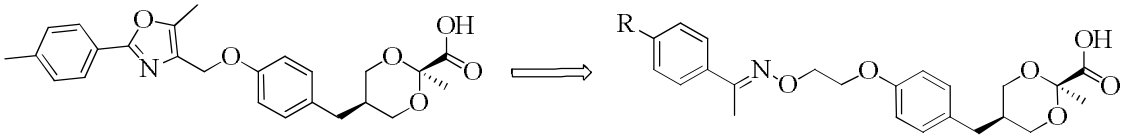

(**I**) (**11**)

Figure 20: Oximes containing 1,3 dioxane-*r*-2-carboxylic acid.

3.1.1.1 Chemistry

With the intention intended to syntheisze the compounds represented by structure **11**. Synthesis methodology was developed based on the

reterosynthetic analysis and the schemes presented below. The methods reported in literature were adapted for the synthesis of **6a** which was the common intemediate for the synthesis of the compounds **11**. Oxime containing fragments were synthesized following the procedures reported earlier, using suitable starting materials and varying reaction conditions, as outlined in schemes and described in experimental sections.

Synthesis of title compounds **11** was achieved as illustrated in **Scheme 1** and **Scheme 2**. Synthesis of key intermediate **6**[225] is outlined in **Scheme 1**. Diester **2** was prepared from **1** by reacting enolate of diethyl malonate. Transformation of **2** to cyclized dioxane **6** (as a mixture of *cis* and *trans* isomers) was achieved by reduction to diol **3** followed by the treatment with methyl pyruvate, in the presence of $BF_3.OEt_2$. The attempts to separate the *cis* and *trans* isomers of **4** by column chromatography were unsuccessful. However separation by recrystallization was successful after debenzylating the mixture of isomers. Pure *cis* isomer **6a** was obtained quantitatively as the first crop whereas *trans* isomer **6b** could be obtained only after repeated crystallizations.

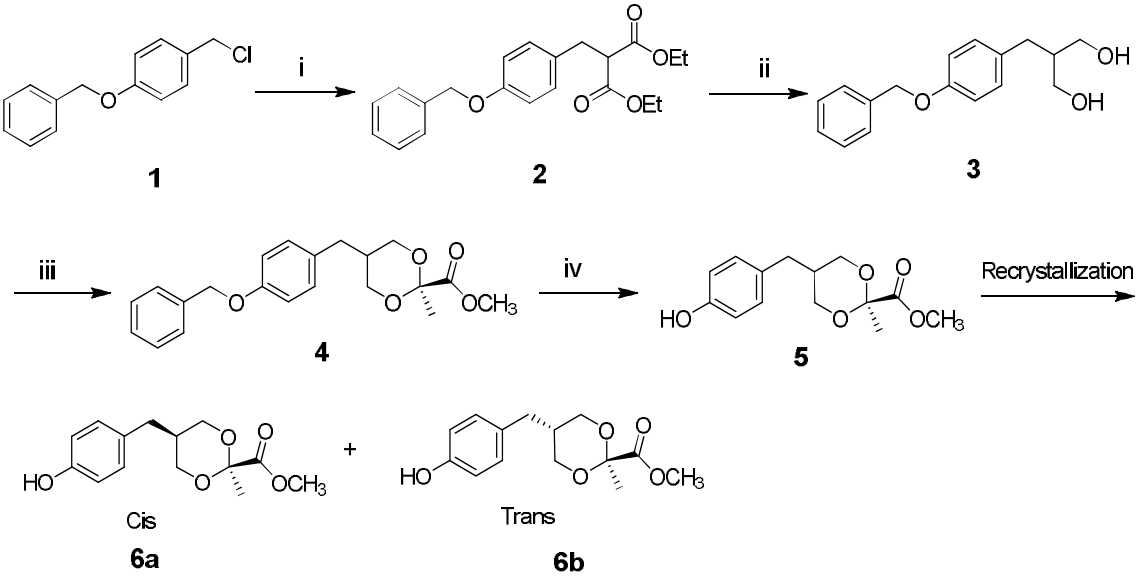

Scheme 1: Reagent and conditions**:** i) Diethyl malonate, NaH (60%), THF, 25 °C, 14 hrs, 79%; ii) LAH, THF, 25 °C, 6 hrs, 39%; iii) Methyl pyruvate, $BF_3.Et_2O$, CH_3CN, 25 °C, 4 hrs, 76%; iv) $HCOONH_4$, Pd/C (10%), CH_3OH, reflux, 2.0 hrs, 95%.

The axial orientation of the carboxyl group in dioxane ring is demonstrated by single crystal X-ray diffraction of the *cis* isomer **6a** (**Figure 21**) and the *trans* isomer **6b** (**Figure 22**). In both the compounds the carboxy group at position-2 is oriented axially, while the benzyl group at 5-positionis oriented equatorially in **6a** and axially in **6b**. These X-ray structures provide conclusive evidence for the preferred axial orientation of carboxyl group due to anomeric effect.

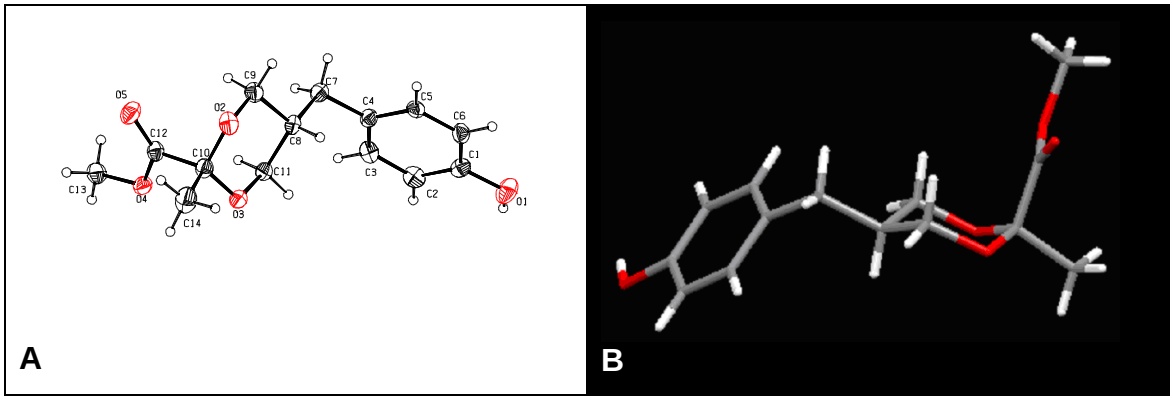

Figure 21: (A) ORTEP diagram of **6a** with atom numbering scheme (30% probability factor for the thermal ellipsoids). (B) (*cis*)

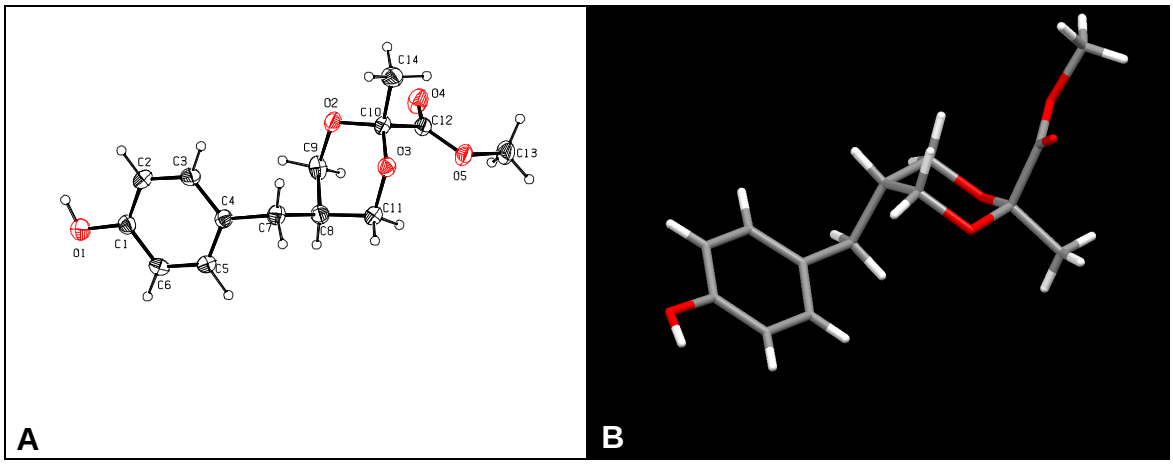

Figure 22: A) ORTEP diagram of **6b** with atom numbering scheme (30% probability factor for the thermal ellipsoids). (B) (*trans*)

Synthesis of **11a-k** is outlined in **Scheme 2**. The oximes (**8a-k**) were synthesized by reacting the corresponding acetophenones (**7a-k**) with hydroxylamine hydrochloride. The geometrical structure of all the oximes (**8a-k**) prepared were considered to be *(E)* because the literature precedent reveals that the *(E)*-isomers are thermodynamically more stable than the corresponding *(Z)*-isomers.[238] Alkylation of oximes (**8a-k**) with 1,2-dibromoethane in the presence of

cesium carbonate (Cs_2CO_3) in dimethylformamide (DMF) gave the intermediates (**9a**-**k**) in good yield. Finally coupling of **9** with **6a**, in the presence of potassium carbonate (K_2CO_3), in DMF gave the esters (**10a-k**), which on hydrolysis under basic condition yielded the desired compounds **11a**-**k**.

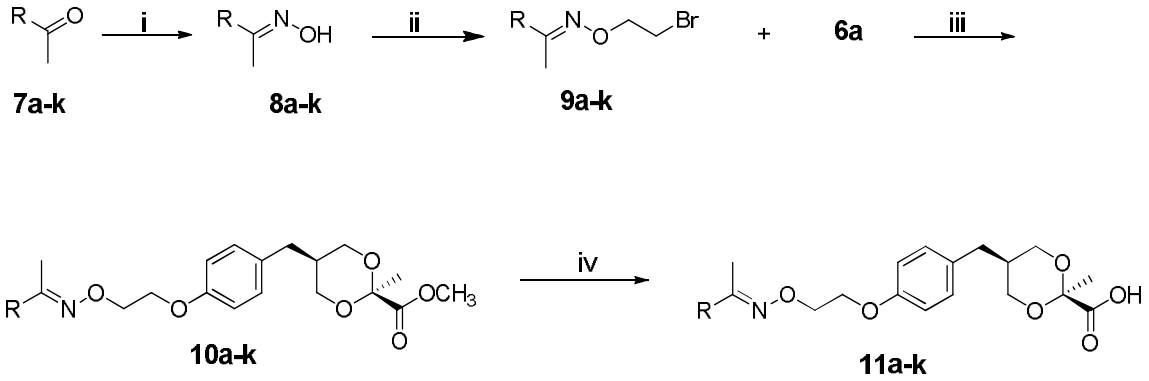

Scheme 2: Reagents and conditions: i) $NH_2OH.HCl$, NaOAc, EtOH, H_2O, reflux, 2 hrs, 48-98%; ii) 1,2-dibromoethane, Cs_2CO_3, DMF, heat, 80 °C, 20 hrs, 19-84%; iii) K_2CO_3, DMF, heat, 80 °C, 20 hrs, 49-93%; iv) $LiOH.H_2O$, CH_3OH, THF, H_2O, 30 °C, 20 hrs, 50-70%.

3.1.1.2 Biology

In order to assess the potency and subtypes selectivity, all the final compounds (**11a-k**) were screened *in vitro* for hPPARα, γ and δ agonistic activities (PPAR transfected in HepG2 cells). The NS-220 (PPARα), GW-501516 (PPARδ), Rosiglitazone (PPARγ) and compound **I** (PPARα/γ) were used as positive controls (standards). As described earlier, the goal was to develop potent and selective PPARα agonist. In this endeavor, the oxazole ring of dual agonist (compound **I**) was replaced with phenyl oxime group (**Figure 20**) and the initial compound **11a** was found to be selective towards PPARα. Based upon the past experience, it was envisioned that substitution at *para*-position of phenyl ring (**11a**) may play important role in the modulation of potency and selectivity of the test compounds. In previous communication it was reported that electron donating groups improve the PPARα selectivity over PPARγ.[239] Thus, substitution at the *para* position of compound **11a** with electron releasing or donating groups showed very good PPARα selectivity over PPARγ, as compounds **11b**, **11c** and **11f** possessing methyl, methoxy and fluoro groups

respectively exhibited excellent potency and selectivity towards PPAR*α* subtype. These findings encouraged the study of the effect of substituents on both 3- and 4-positions of the phenyl ring. In this regard, compound **11d** with methoxy group on both the positions was synthesized but it failed to retain its selectivity as well as potency. Substitution at *para* position with electron withdrawing groups exhibited detrimental effects *in vitro*, as evident from the activity results of **11e, 11g** and **11h** possessing methane sulfonyl, trifluoromethyl and trifluoromethoxy groups respectively. Surprisingly compound **11h** showed PPARγ selectivity over PPARα. Furthermore, when the flexible substitution at para-position was replaced with a rigid bi-cyclic ring systems (tetrahydronaphthyl (**6i**) and naphthyl (**11j**)), it resulted into weak agonistic activity and poor affinity towards all subtypes tested. Similarly, compound **11k** prepared by replacing phenyl ring with 3-pyridyl ring showed weaker agonistic activity as compared with **11a**. Together, these *in vitro* agonistic activity results across all the three PPAR subtypes clearly confirmed the hypothesis that the phenyl oxime group act as a bioisostere of oxazole ring system. Furthermore, structure activity relationship (SAR) drawn from the *in vitro* study results indicated that electron donating groups at para position of the phenyl ring are essential for PPARα selectivity. These results demonstrate the viablity of the selected approach towards developing novel PPARα agonists. The *in vitro* activity results (fold inductions Vs vehicle control (DMSO; 1% solution)) are summarized in **Table 8**.

Table 8. *In vitro* hPPAR transactivation activity of test compounds (**11a-k**).

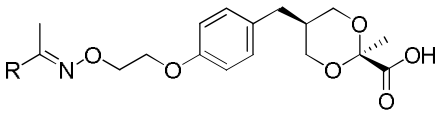

Compound	R	hPPAR Transactivation[a]		
		α^b(10μM)	γ^b(0.2μM)	δ^b(10μM)
11a	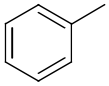	10.79	1.47	1.58
11b	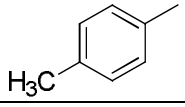	10.81	3.05	2.78

Compound	R	hPPAR Transactivation[a]		
		α^b(10μM)	γ^b(0.2μM)	δ^b(10μM)
11c	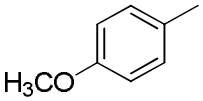	15.04	1.44	IA
11d	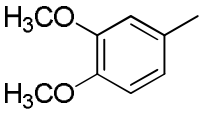	3.61	1.75	1.68
11e	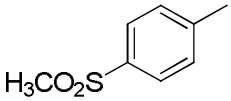	1.37	IA	1.23
11f	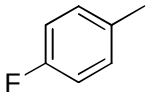	10.49	1.20	1.62
11g	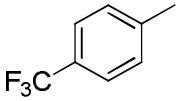	5.79	2.83	1.31
11h	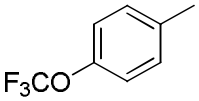	3.48	7.39	1.46
11i	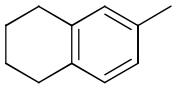	1.63	4.36	1.25
11j	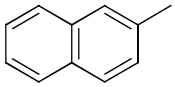	1.76	3.87	IA
11k	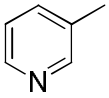	2.36	1.13	1.31
Vehicle (DMSO)		1.0	1.0	1.0
I		14.72	7.90	IA
NS-220		12.72	IA	2.52
GW-501516		ND	ND	9.24
Rosiglitazone		IA	7.22	IA

[a] IA denotes inactive where compounds did not show any fold activation above basal level shown by vechile and ND denotes not detemined. hPPAR denotes human PPAR.

[b] Activites are presented as fold induction of PPARα, γ and δ activation over basal level (DMSO).

Based on the *in vitro* results, the *in vivo* antihyperlipidemic and antihyperglycemic activities of the lead compound **11c** (a highly potent and PPAR*α* selective *in vitro*) were evaluated in *db/db* mice. In this model, mice were dosed orally with either compound **11c** or positive control (**NS-220**) at 3 and 30 mpk (mg/kg/day) for 7 days and serum triglycerides (TG) and serum glucose (Glucose) were measured. As shown in **Table 9**, compound **11c** showed

significant reduction in TG and glucose, comparable to positive control (**NS-220**), at 10-fold lower dose.

Table 9. *Anti*-hyperlipidemic and *anti*-hyperglycemic activities of compound **11c** in *db/db* mice[a].

Compd	Dose (mg/kg/day)	% Change	
		TG	Glucose
11c	3	-53	-45
NS-220	30	-54	-43

[a] Values indicated are the mean of n= 6 and $p < 0.05$ vs vehicle control.

Similarly, in high cholesterol fed *Sprague Dawley* rats (HC fed SD rat), compound **11c** exhibited excellent reduction in TG, total cholesterol (TC) and LDL-cholesterol (LDL-C), along with increase in the levels of HDL-cholesterol (HDL-C). As observed in *db/db* mice, compound **11c** showed comparable antihyperlipidemic activity in HC fed SD rat at 10-fold lower dose (**Table 10**).

Table 10. *In vivo anti*-hyperlipidemic activity of compound **11c** in HC fed SD rats[a].

Compd	Dose (mg/kg/day)	% Change			
		TG	TC	LDL-C	HDL-C
11c	3	-54	-56	-68	68
NS-220	30	-51	-49	-58	62

[a] Values indicated are the mean of n= 9 and $p < 0.05$ vs vehicle control.

Further to assess the rational behind superior *in vivo* efficacy of compound **11c** over **NS-220**, single dose (30 mg/kg/day, oral) comparative pharmacokinetic study was carried out in male *wistar* rats. The compound **11c** showed rapid Tmax, high Cmax and AUC, along with extended half-life. Compared to **NS-220**, compound **11c** showed 3-fold higher Cmax, 14-fold improvement in AUC and 7-fold longer half-life. Thus, improved pharmacokinetic profile of compound **11c** justifies its excellent pharmacodynamic effects in animal models at a lower dose. The results are summarized in **Table 11.**

Table 11. Mean pharmacokinetic parameters[a] of **11c** in fasted male *wistar* rats.

Compd	T_{max} (h)	C_{max} (ng/ml)	$T_{1/2}$ (h)	AUC (0-α) (h ng/ml)
11c	0.61±0.02	119.61±1.01	13.96±1.91	1420.01±18.31
NS-220	0.65±0.10	40.32±1.19	1.99±0.76	99.96±11.41

[a] Values indicate mean ± SD for n=6

3.1.1.3 Molecular docking study

The molecular docking analysis of **11c** was carried out to infer its selectivity at molecular level and to locate critical interactions with the active site of PPAR*α* and PPARγ binding pockets, using Glide version 5.6. Briefly, the automated docking program implemented in the Schrodinger package. The geometry of docked compound (**11c**) was subsequently optimized using the LigPrep version 2.6. The complexed X-ray crystal structure of the ligand binding domain (LBD) of PPARα with GW409544 (1K7l.pdb) and PPARγ with Rosiglitazone (2PRG.pdb) were obtained from RCSB Protein Data Bank. As depicted in **Figure 23**, when **11c** was docked into PPARα binding pocket, the most stable docking models of **11c** adopted a conformation that allows the carboxylic group to form hydrogen bonds with Tyr314, Tyr464, and Ser280 (**Figure 23; A**), which have been reported to be essential interaction for PPARα selective compounds.[240] The literature precedence suggests that interaction of the ligand with Ser289, His323, Tyr473 and His449 are important for PPARγ affinity, as this H-bonding network could stabilize the AF-2 helix in a conformation which favors the binding of co-activators to PPARγ and consequently, enhance their recruitment. When **11c** was docked into PPARγ binding pocket the most stable docking model of **11c** adopted a conformation that only allows the carboxylic group to form hydrogen bonds with Tyr473 and Ser289. However, other important residues such as His449 and His323 which are crucial for PPARγ selectivity were found to be away from the ligand and no H-bond interactions of

these amino acids with the carboxylate group of compound **11c** were observed (**Figure 23; B**).

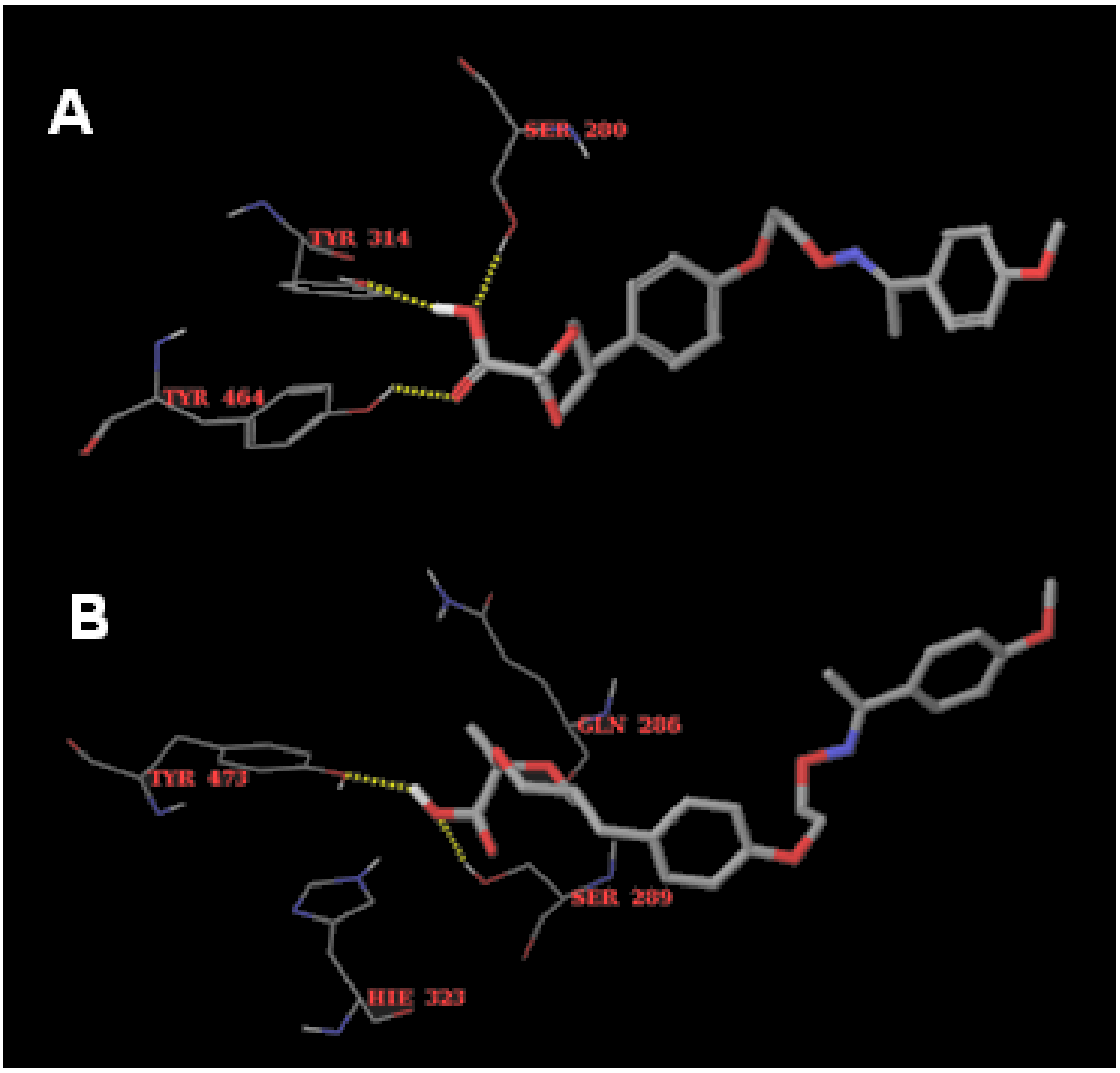

Figure 23: Molecular docking of **11c** into PPARα (**A**) and γ (**B**) binding pockets:H-bond interactions with amino acids are shown in dashed lines.

Thus favorable *in-silico* interaction of compound **11c** with PPAR*α* binding pocket and partial interaction with PPARγ binding pocket might correlate its *in vitro* selectivity profile toward PPAR*α* over PPARγ.

3.1.2 Structure-Activity Relationship of indole containing benzyl 1,3-dioxane-*r*-2-carboxylic acid derivatives, a novel class of subtype selective PPARα agonist

Results from earlier series, encouraged us to study the structure activity releationship of compound **III** by replacing the oxazole moiety with optimized indole group as lipophilic tail (based on a known compound DRF 2189) and the compound **III** showed selectivity towards PPARα.[228] A medicinal chemistry effort was initiated based on the interesting biological profile of lead compound **III**. Herein, the effect of chemical diversity at the 5-position of the phenyl group of indole scaffold of lead compound **III** (**Figure 24**), was investigated based on litreature precidences.[241-244] Finally, azoindole group was used as lipophilic group to create further chemical diversity by incorporating a hetero atom, nitrogen in the indole core.

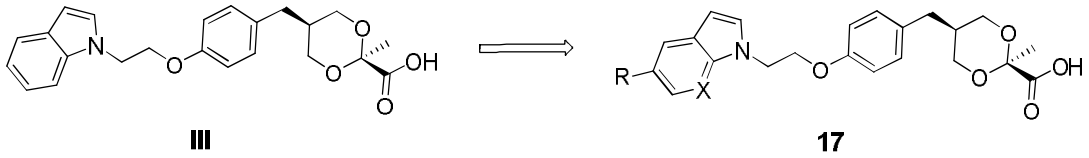

Figure 24: Structure-Activity Relationship of 5-substituted indole.

3.1.2.1 Chemistry

For the synthesis of **17a–i**, the compounds (**13a-g** and **13i**) were prepared by alkylating commercially available 5-substiuted indole (**12a-g** and **12i**) in dimethylformamide with ethyl bromoacetate using sodium hydride as a base. The resulting esters (**13a-g** and **13i**) were reduced with lithium aluminum hydride, in tetrahydrofuran to yield desired alcohols (**14a-g** and **14i**). Alcohols (**14a-g** and **14i**) were treated with methane sulfonyl chloride and triethylamine, in dichloromethane to yield mesylate compounds (**15a-g** and **15i**). Coupling reaction of (**15a-g** and **15i**) with **6a**, in the presence of cesium carbonate in dimethylformamide gave esters (**16a-g** and **16i**), which on hydrolysis under aqueous basic condition yielded carboxylic acids (**17a-g** and **17i**). Debenzylation

of **17g** was carried out using palladium carbon and ammonium formate, in methanol (hydrogenation) to furnished **17h** (**Scheme 3**).

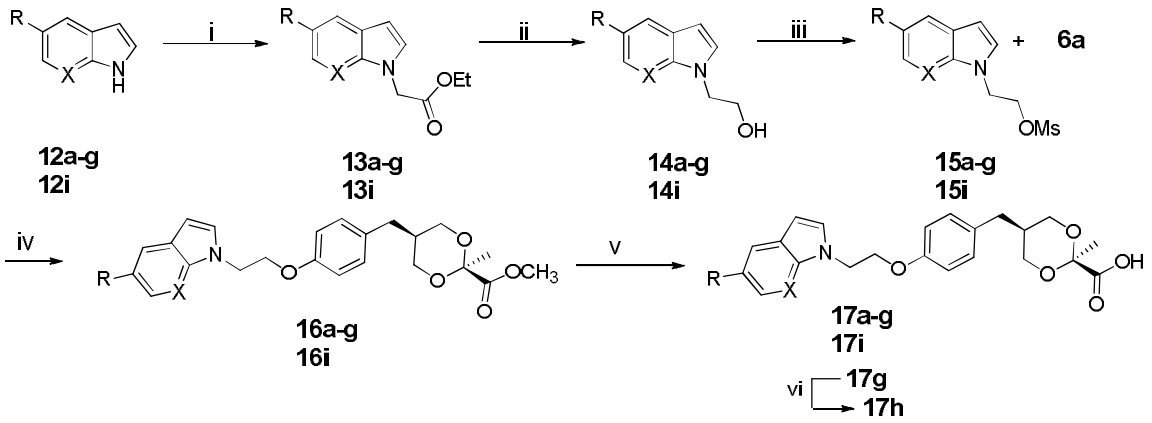

17a) X = CH, R = CH_3 ; **17b**) X = CH, R = OCH_3 ; **17c**) X =CH, R = F; **17d**) X =CH, R = Cl;
17e) X = CH, R = Br; **17f**) X =CH, R = NO_2; **17g**) X = CH, R = OBn; **17h**) X =CH, R = OH; **17i**) X = N, R = H.

Scheme 3: Reagents and conditions: i) Ethyl bromoacetate, NaH, THF, 30 °C, 20-24 hrs: ii) LAH, THF, 25 °C, 6.0 hrs, 10-64%; iii) CH_3SO_2Cl, Et_3N, CH_2Cl_2, 30 °C, 0.5-2.0 hrs, 40-100%; iv) Cs_2CO_3, DMF, 60°C, 18-24 hrs, 60-87%; v) $LiOH.H_2O$, THF: CH_3OH: H_2O, 25°C, 4.0-5.0 hrs, 49-85%; vi) H_2, Pd/C,$HCOONH_4$, methanol, reflux, 2.0 hrs, 49%.

3.1.2.2 Biology

All the final compounds synthesized (**17a–i**) were screened *in vitro* for PPAR*α*, *γ* and *δ* agonistic activities in PPAR receptor transfected HepG2 cells according to the procedure described earlier. NS-220, Rosiglitazone and GW501516 were used as positive controls (standards) for PPAR*α*, *γ* and *δ* respectively. As described earlier, our initial goal was to investigate the effect of chemical diversity on 5-position of phenyl group of the indole scaffold, of the lead compound **III**. The previous experience suggested that electron donating group on aromatic part of the lipophilic group increase the PPAR*α* activity and selectivity. The first approach was to study the effect of electron releasing or donating groups on PPAR agonistic activity. Compound **17a** (R = CH_3) and **17b** (R = OCH_3) were found to be potent towards PPAR*α* over PPAR*γ* and PPAR*δ*. Compared with the compound **III**, **17a** showed excellent potency towards PPAR*α*. When Compounds were substituted with halogen (**17c-e**), PPAR*α* activity reduced from **17c** (small size and strong electron withdrawing fluoro) to

17e (large size and weak electron withdrawing bromo). But when compound was substituted with very strong electron withdrawing nitro group, compound **17f** exhibited an excellent activity towards PPAR*α*. Thus the result suggests that the electronic effects of substituted groups influence the charge distribution in the lipophilic tail and the interaction between compounds and PPAR receptors. Further, it was planned to study the effect of size of the substituents on PPAR agonistic activity, as expected, compound **17g** with bulkier benzyloxy group increased the activity of PPARγ and reduced the PPAR*α* activity, mainly because the ligand binding pocket of PPARγ is bulkier than that of PPAR*α*. Compound **17g** behaved as PPAR*α*/γ dual agonist. While compound **17h** with smaller hydroxyl group showed detrimental effect toward all PPAR subtypes. The next approach was to create further chemical diversity by incorporating azoindole group as lipophilic tail as in compound **17i** in which PPAR*α* activity was marginally reduced compared to compound **III**. Furthermore, Structure–Activity Relationship (SAR) drawn from the *in vitro* study results indicated that chemical diversity on 5-position of phenyl group of the indole scaffold influence the selectivity of PPAR*α* over PPARγ and PPAR*δ*. The *in vitro* activity results (fold induction Vs vehicle control (DMSO; 1 % solution)) are summarized in **Table 12**.

Table 12. *In vitro* hPPAR transactivation activity of compounds **17a-i**.

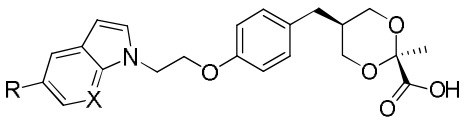

Compound	R	X	hPPAR Transactivation[a]		
			α^b (10μM)	γ^b (0.2μM)	δ^b (10μM)
17a	CH_3	CH	16.0	1.24	2.05
17b	OCH_3	CH	12.23	1.89	1.57
17c	F	CH	10.39	2.03	1.81
17d	Cl	CH	9.40	2.31	1.79

Compound	R	X	hPPAR Transactivation[a]		
			α^b (10μM)	γ^b (0.2μM)	δ^b (10μM)
17e	Br	CH	8.80	1.50	0.92
17f	NO_2	CH	13.29	1.14	1.35
17g	OBn	CH	6.80	8.82	1.01
17h	OH	CH	2.16	IA	1.41
17i	H	N	8.20	IA	1.44
III	H	CH	10.13	1.27	1.09
Vehicle (DMSO)			1.0	1.0	1.0
NS-220			12.72	IA	2.52
Rosiglitazone			IA	7.22	IA
GW-501516			ND	ND	9.24

[a] IA denotes inactive where compounds did not show any fold activation above basal level shown by vechile and ND denotes not detemined. hPPAR denotes human PPAR.

[b] Activites are presented as fold induction of PPARα, γ and δ activation over basal level (DMSO).

Based on the *in vitro* results, compound **17a**, (potent PPAR*α* agonist), **17g** (PPAR*α*/γ dual activator) and **17i** (PPAR*α* agonist with structural resemblance to **III**) were selected for *in vivo* evaluation in *db/db* mice. NS-220 and Fenofibrate were used as reference standards.The compounds (**17a, 17g** and **17i**) were administrated at the dose of 3 mg/kg/day, NS-220 was administrated at the dose of 30 mg/kg/day and Fenofibrate was administrated at the dose of 300 mg/kg/day, orally to *db*/*db* mice for 7 days. Compound **17a** showed 51.7% reduction of elevated triglyceride and 48.9 % reduction of glucose, which was found to be comparable to NS-220, even at 10 times lower dose than NS-220 and superior to Fenofibrate even, at 100 times lower dose than Fenofibrate. **17g** and **17i** also exhibited excellent reduction in elevated triglyceride 38.5% and 37.4 % respectively, with improving the glucose reduction.The results are summarized in **Table 13**.

Table 13. *In vivo* efficacy of the compound **17a**, **17g** and **17i** in *db/db* mice[a]

Compound	Dose (mg/kg/day)	% Change Vs Control	
		TG	Glucose
17a	3	-51.7	-48.9
17g	3	-38.5	-30.6
17i	3	-37.4	-14.9
NS-220	30	-54.0	-43.0
Fenofibrate	300	-36.6	-35.5

[a] Values indicated are the mean of n= 6 and $p < 0.05$ vs vehicle control.

Overall data suggest that indole based benzyl 1,3-dioxane-*r*-2-carboxylic acid derivatives exhibited potent hPPAR*α* activity and successfully reduced serum triglyceride and glucose *in vivo*.

3.1.2.3 Molecular docking study

To further understand the activity and selectivity profile of compound **17a** at molecular level, docking studies were carried out for this compound using Glide version 6.7. The complexed X-ray crystal structure of the ligand binding domain (LBD) of PPARα with AZ 242 (1I7G.pdb), PPARγ with Rosiglitazone (2PRG.pdb) were obtained from RCSB Protein Data Bank. When docked into PPARα binding pocket the most stable docking models of **17a** adopted a conformation that allows the carboxylic group to form hydrogen bonds with Tyr464, His440 and Ser280. Other important residue Tyr314 is also close to the ligand. While in PPARγ binding pocket the carbonyl of carboxylic group forms hydrogen bond only with hydroxyl of Ser289. Other important reported residues Tyr473, Gln286 and His323, are little bit away from ligand. In the light of these docking calculations, it can be inferred that **17a** could be more selective towards PPARα rather than PPARγ (**Figure 25**).

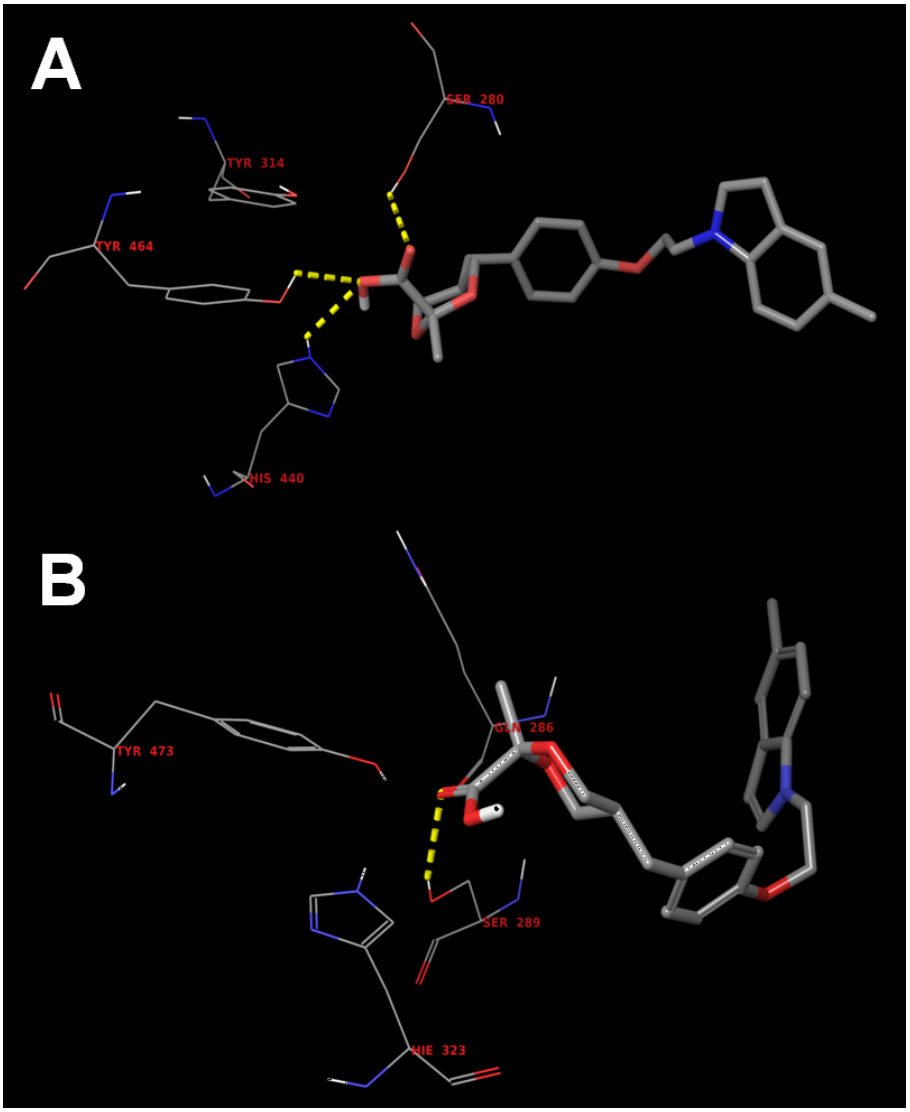

Figure 25: Molecular docking of **17a** into PPARα (**A**) and γ (**B**) binding pockets: H-bond interactions with amino acids are shown in dashed lines.

3.2 Design and synthesis of weak and partial PPARα selective agonists.

NS-220 is very potent and selective PPAR*α* agonist containing the 1,3-dioxane-*r*-2-carboxylic acid as an acidic head, was found to very efficacious in reducing both glucose and lipid.[226] Though this compound is very potent and efficacious, its development was discontinued for unknown reasons. It is believed that the high potency of this compound could be posible reason for its failure. Therefore it was intended to synthesize the compounds with weak *in vitro* potency and desired *in vivo* efficacy. To meet these objectives, it was decided to optimize the lipophilic portion of compound **V**.

Thus, it was planned to investigate the effect of substitutions on *para*-positions of the phenyl groups of lipophilic part with groups having different electronic and steric properties. Initially it was intended to synthesize the compounds **22a-j**. Based on the *in vitro* and *in vivo* results of derivatives **22a-j** the compound **22a-j** to **27a-e** were modified with ring equivalent bioisosteric replacement on lipophilic tail by replacing phenyl with pyridyl group and finally the compound **33a-b** were synthesized by replacing the oximino group with olefin, as depicted in **Figure 26**.

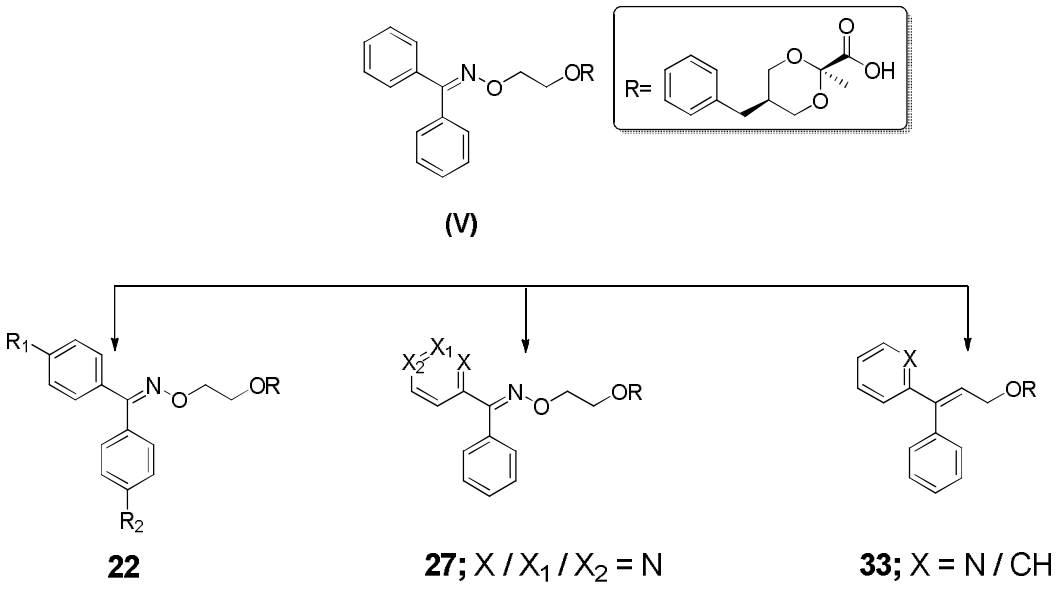

Figure 26: Structural modifications in the lipophilic tail region.

3.2.1 Chemistry

Synthesis of the compounds **22a-j** was carried out as outlined in **Scheme 4**. *p*-Substituted benzophenone oximes (**19a-c** & **19e-j**) were synthesized by refluxing the corresponding benzophenone (**18a-c** & **18e-j**), with hydroxylamine hydrochloride and sodium acetate, in a mixture of ethanol and water. In case of the compounds (**19a-c** and **19e**), mixtures of the two isomers (*E* and *Z*) were obtained due to substitution on one of the phenyl ring and were directly used further, without separation. Alkylation of the oximes (**19a-c** and **19e-j**), with excess of 1,2-dibromoethane in the presence of cesium carbonate in dimethyl formamide (DMF) gave the intermediates **20a-c** and **20e-j** respectively, in good yield. Excess amount (10 fold) of 1,2-dibromoethane was used to avoid dimerization. The coupling reaction of **20a-c** and **20e-j** with **6a**[225], in the presence of potassium carbonate (K_2CO_3) in DMF at 80 ^oC gave the esters **21a-c** and **21e-j** respectively. Compound **21c** was oxidized with ®Oxone in a mixture of water and acetone to get **21d**. Finally the compounds **22a-j** were obtained by the hydrolysis of their respective esters (**21a-j**), under basic conditions. Compounds **22a-e** were obtained as a mixture of *E* and *Z* isomers (**Scheme 4**).

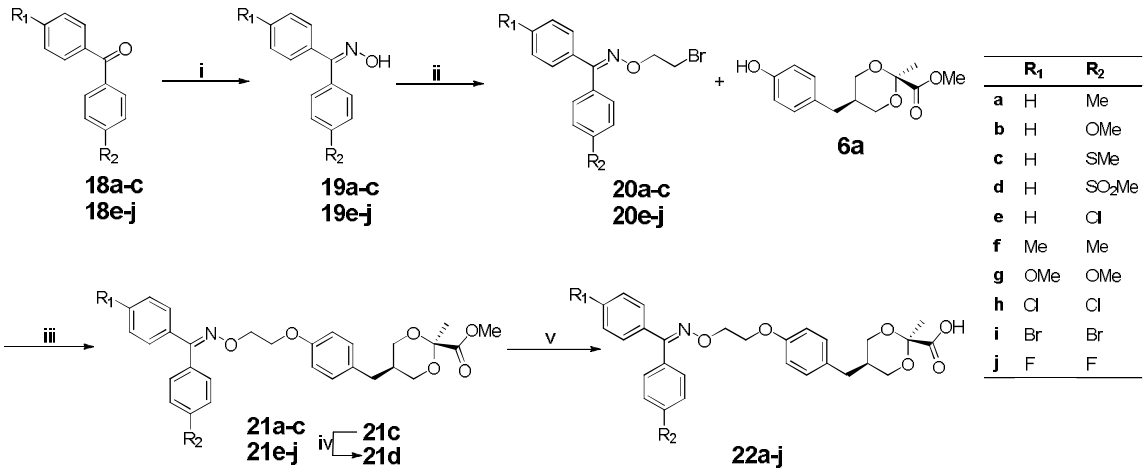

	R_1	R_2
a	H	Me
b	H	OMe
c	H	SMe
d	H	SO_2Me
e	H	Cl
f	Me	Me
g	OMe	OMe
h	Cl	Cl
i	Br	Br
j	F	F

Scheme 4. Reagents and conditions: i) $NH_2OH.HCl$, NaOAc, EtOH : H_2O, reflux, 20-24 hrs, 61-100%; ii) Cs_2CO_3, 1,2-Dibromoethane, 80 ^oC, 40 hrs, 41-96%; iii) K_2CO_3, DMF, 80 ^oC, 18-24 hrs, 50-90%; iv) Oxone, acetone : water (1:1), 27 ^oC, 3 hrs, 83%; v) $LiOH.H_2O$, THF, H_2O, MeOH, 30 ^oC, 12-18 hrs, 62-93%.

For the synthesis of the compounds **27a-e** treatment of benzoylpyridines **23a-c** with hydroxylamine hydrochloride and sodium acetate in a mixture of ethanol and water (following the step shown in Scheme 1) gave the oxime derivatives **24a-c**, as a mixture of *E* & *Z* isomers. Treatment of **24a-c** with 1,2-dibromoethane gave compound **25a-e**. Separation of the isomer **25a-d** was accomplished by column chromatography while the compound **25e** could not be separated. Finally, coupling of **25a**-**e** with **6a**, in the presence of K_2CO_3 in DMF gave the ester **26a**-**e**, which on hydrolysis under basic condition yielded compounds **27a**-**e** (**Scheme 5**).

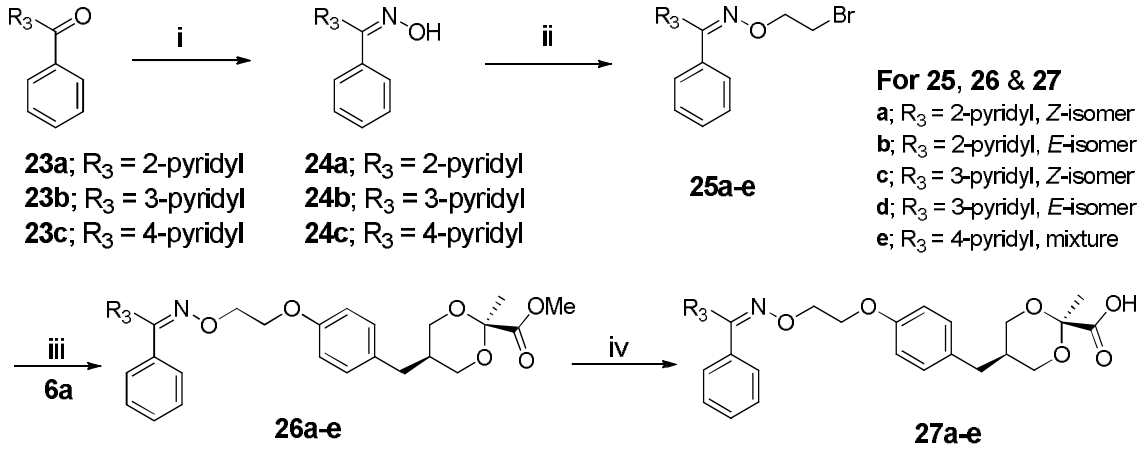

Scheme 5. Reagents and conditions: i) $NH_2OH.HCl$, NaOAc, EtOH : H_2O, reflux, 20-24 hrs, 78-100%; ii) Cs_2CO_3, 1,2-Dibromoethane, 80 ^oC, 40 hrs, 10-50%; iii) K_2CO_3, DMF, 80 ^oC, 18-24 hrs, 43-72%; iv) $LiOH.H_2O$, THF, H_2O, MeOH, 30 ^oC, 12-18 hrs, 51-92%.

Further to establish the *cis* configuration in 1,3-dioxane ring and geometrical isomerism around C=N bond in compounds **27**, single crystals of **27a** and **27b** were grown and subjected for single crystal X-ray diffraction. The results provided conclusive evidence for the preferred axial orientation of carboxyl group in dioxane ring due to anomeric effect and also confirmed *E* and *Z* configuration of the oxime (**Figure 27**).

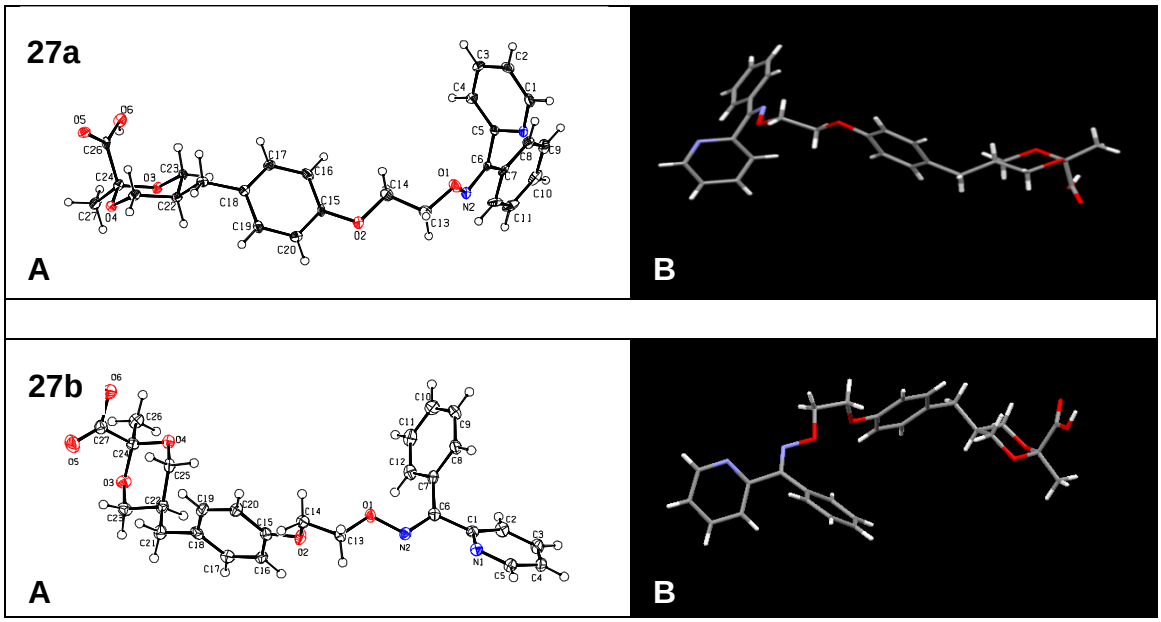

Figure 27: Structure of **27a** and **27b** determined by single crystal X-ray diffraction: (A) ORTEP diagram with atom numbering scheme (B) Image generated by Mercury software 2.3 version.

For the synthesis of compounds **33a-b** Horner Emmons reaction on commercially available benzophenone (**28**) and 2-benzoylpyridine (**23a**) with triethyl orthophosphanoacetate and sodium hydride in THF, led to the formation of intermediates **29a** and **29b-c** respectively. The *E* isomer **29b** and the *Z* isomer **29c** were separated from the mixture by column chromatography and the stereochemistry was assigned using ^{1}H NMR. Reduction of the esters (**29a-c**) carried with DIBAL-H in THF yielded the alcohols **30a** and **30b** from their respective esters but unfortunately, reduction of **29c** failed to give the desired product under the same reaction condition. Mesylate **31a-b**, were prepared by reacting the corresponding alcohols (**29a-b**) and methanesulfonyl chloride, in the presence of triethyl amine. Compounds **31a-b** was subsequently subjected to a nucleophilic substitution reaction with **6a** to get the esters (**32a-b**)**.** Hydrolysis of these esters produced the desired products **33a-b** (**Scheme 6**).

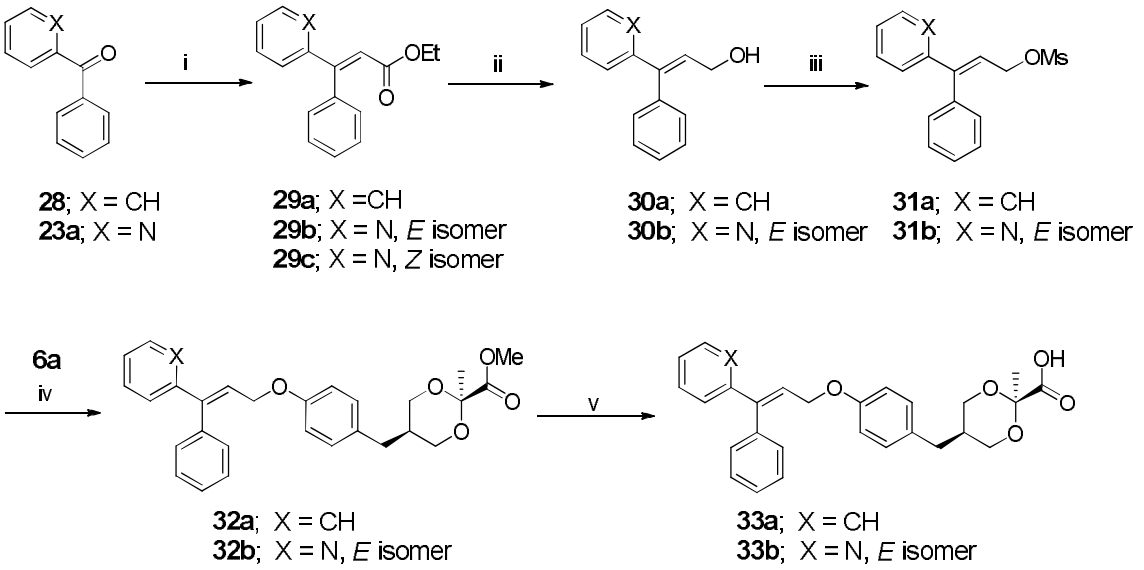

Scheme 6. Reagents and conditions: i) Triethyl phosphanoacetate, NaH (50%), THF, 30 ^{o}C, 70 hrs, 28-56%; ii) DIBAL-H, THF, 30 ^{o}C, 0.5 hr, 87-91%; iii) MsCl, Et_3N, CH_2Cl_2, 30 ^{o}C, 0.5-2.0 hrs, 100%; iv) K_2CO_3, DMF, 80 ^{o}C, 18-24 hrs, 29-51% ; v) $LiOH.H_2O$, THF, H_2O, MeOH, 30 ^{o}C, 12-18 hrs, 68-95%.

3.2.2 Biology

All the final compounds (**22a-j**, **27a-e** and **33a-b**) synthesized were screened *in vitro* for PPAR*α*, *γ* and *δ* agonistic activities, in PPAR receptor transfected HepG2 cells. WY-14643, Rosiglitazone and GW501516 were used as positive controls (standards) for PPAR*α*, *γ* and *δ* respectively. Based on the fold induction results, hPPAR*α* EC_{50} (half maximal effective concentration) and E_{max} (% Effect of compound was compared to standard) of selected compounds were determined. Based on suitable *in vitro* profiles, selected compounds were screened *in vivo* for triglyceride lowering efficacy, in male *Swiss albino mice* (SAM) at dose of 10 mg/kg/day for 6 days and Fenofibrate was used as a standard at dose of 300 mg/kg/day.

To study the structure-activity relationship (SAR) of compound **V**, initially mono-substituted analogues (**22a-e**) were synthesized by substituting at metabolically susceptible *para* position of the phenyl group of the oxime, with groups having diverse electronic and steric effects, mainly because *para* position of phenyl ring of tail part may play important role in the modulation of potency

and selectivity of the compounds and the results are described in **Table 14**. The *in vitro* activities of these compounds were found to be very sensitive to the substitution at *para*-position. Compounds **22b** and **22c** with electron donating methoxy and methane sulfanyl groups respectively were found to be potent PPAR*α* agonist ((αEC_{50} = 0.63 µM, E_{max} = 158%), (αEC_{50} = 0.18 µM, E_{max} = 154% respectively) but *in vivo* did not show significant reduction of serum triglyceride *in SAM.* Whereas, compound **22a** with methyl group found to be moderate activator of PPAR*α* and PPAR*γ.* Finally, substitution with large size methane sulfonyl group (**22d**) and small size chlorine (**22e**) group (as in fibrates) showed detrimental effect towards PPAR*α*.

Table 14. *In vitro* hPPAR transactivation and TG reducing activity of **22a-j**.

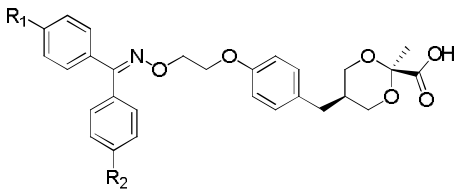

Compd	R_1	R_2	hPPAR Transactivation[a]					% Change in serum TG[e]
			α^b (10µM)	γ^b (0.2µM)	δ^b (10µM)	α^c %E_{max}	α^d EC_{50} (µM)	
22a	H	CH_3	4.83	2.30	1.30	ND	ND	ND
22b	H	OCH_3	10.83	1.16	IA	158	0.63	-21.9
22c	H	SMe	8.18	1.17	1.02	154	0.18	-20.4
22d	H	SO_2CH_3	2.38	IA	1.06	ND	ND	ND
22e	H	Cl	3.38	1.79	1.51	ND	ND	ND
22f	CH_3	CH_3	5.64	2.23	1.74	ND	ND	ND
22g	OMe	OMe	12.79	1.73	1.08	177	0.22	-27.6
22h	Cl	Cl	IA	IA	IA	ND	ND	ND
22i	Br	Br	IA	1.23	IA	ND	ND	ND
22j	F	F	9.61	IA	IA	158	0.32	-11.6
V	H	H	16.28	IA	ND	181	0.14	-46.0
IV			14.62	3.49	1.49	ND	0.0002	-9.0

Compd	R_1	R_2	hPPAR Transactivation[a]					% Change in serum TG[e]
			α^b (10μM)	γ^b (0.2μM)	δ^b (10μM)	α^c $\%E_{max}$	α^d EC_{50} (μM)	
I			8.24	3.60	1.27	ND	0.072	-39.0
Fenofibrate			6.58	IA	1.51	90	10.8	-36.6[f]
Vehicle			1.0	1.0	1.0			
WY-14643			7.31	ND	ND	100	1.88	
Rosiglitazone			IA	3.90	IA			
GW-501516			ND	ND	6.73			

[a]IA denotes inactive where compounds did not show any fold activation above basal level shown by vehicle (DMSO) and ND denotes not detemined. hPPAR denotes human PPAR.
[b]Activites are presented as fold induction of PPARα, γ and δ activation over basal level (DMSO).
[c]% *E*max (maximal efficacy) of all test compounds was compared to WY14643 (100% PPARα).
[d] EC_{50} is half maximal effective concentration.
[e]Values indicated are the mean of n= 6 and $p < 0.05$ vs vehicle control.
[f]Fenofibrate was administered orally at a dose of 300 mg/kg/day.

To find out the effect of identical substitution at both R_1 and R_2 position, *bis*-substituted analogues were synthesized by selecting methyl (**22f**), methoxy (**22g**) and chlorine (**22h**) groups. As shown in **Table 14**, compound **22f** and **22g** (αEC_{50} = 0.22 μM, E_{max} = 177%) displayed nearly similar potency compared to their mono-substituted counterpart, whereas compound **22h** was found to be inactive towards all PPAR subtypes. Compound **22g** reduced serum triglycedride by 27% *in vivo*. To further confirm the electronic and steric effect of small halides on PPAR subtype selectivity, we synthesized two more halo group substituted analogues (**22i-j**). One is large size and weak electron withdrawing bromo group (**22i**) and another is much small size and strong electron withdrawing fluoro group (**22j**), compare to chloro group. The result showed that compound with large size bromo group (**22i**) was found inactive towards all PPAR subtypes. Unexpectedly, compound **22j** with small size fluoro group found to be potent PPAR*α* (αEC_{50} = 0.32 μM, E_{max} = 158%) but this compound is not efficacious in reducing TG *in vivo.* All the test compounds (**22a-j**) exhibited low potency towards PPAR*α* compared to potent PPAR*α* activator (**V**).

In vitro results encouraged us to study another series, in which, the phenyl group of compound **III** was bioisosterically replaced with pyridyl group, to get the compounds having 2-pyridyl (**27a**, *Z* isomer and **27b**, *E* isomer), 3-pyridyl (**27c**, *Z* isomer and **27d**, *E* isomer) and 4-pyridyl (**27e**, *Z* and *E* isomer mixture). Both the isomers **27a** and **27b** possessing 2-pyridyl ring system found to be weak and partial activator of hPPAR*α* and compound **27a** is more potent hPPAR*α* agonist (αEC_{50} = 7.98 µM, E_{max} = 50%) compared to **27b** (αEC_{50} = 19.89 µM, E_{max} = 52%) (**Figure 28**). Compound **27a** exhibited similar agonistic activity in mPPAR*α* (αEC_{50} = 2.96 µM, E_{max} = 38%). Compound **27c** and **27d** exhibited poor activity towards PPAR*α* and PPAR*δ* and compounds **27e** found to be inactive towards PPAR subtypes (**Table 15**).

Table 15. *In vitro* hPPAR transactivation and TG reducing activity of **27a-e**.

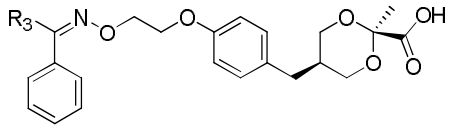

Compd	R_3	Isomer	hPPAR Transactivation[a]					% Change in serum TG[e]
			α[b] (10µM)	γ[b] (0.2µM)	δ[b] (10µM)	α[c] % E_{max}	α[d] EC_{50} (µM)	
27a	2-pyridyl	*Z*	3.88	IA	1.22	50	7.98	-44.0
27b	2-pyridyl	*E*	2.68	IA	1.39	52	19.9	-46.5
27c	3-pyridyl	*Z*	1.31	IA	1.19	ND	ND	ND
27d	3-pyridyl	*E*	1.42	IA	1.23	ND	ND	ND
27e	4-pyridyl	*E,Z*	1.20	IA	1.03	ND	ND	ND
V			16.28	IA	ND	181	0.14	-46.0
Fenofibrate			6.58	IA	1.51	90	10.8	-36.6[f]

[a]IA denotes inactive where compounds did not show any fold activation above basal level shown by vehicle (DMSOand ND denotes not detemined. hPPAR denotes human PPAR.
[b]Activites are presented as fold induction of PPARα, γ and δ activation over basal level (DMSO).
[c]% *E*max (maximal efficacy) of all test compounds was compared to WY14643 (100% PPARα).
[d] EC_{50} is half maximal effective concentration.
[e]Values indicated are the mean of n= 6 and $p < 0.05$ vs vehicle control.
[f]Fenofibrate was administered orally at a dose of 300 mg/kg/day

To the surprise, in spite of their weak and partial *in vitro* agonistic activity, compounds **27a** and **27b** reduced serum triglyceride by 44% and 46.5% respectively in *SAM* which is comparable to **V** and superior to fenofibrate.

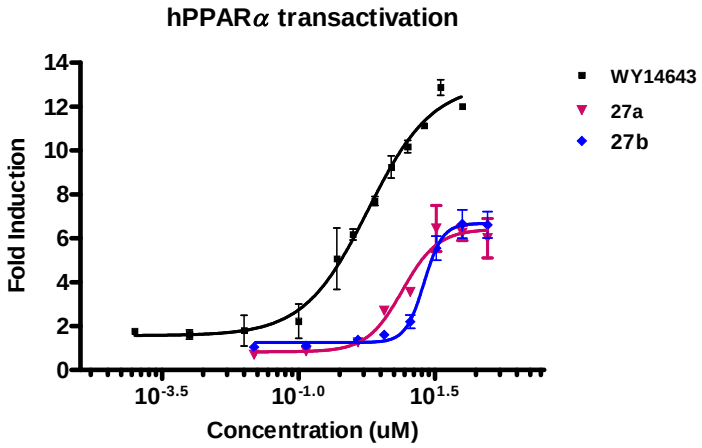

Figure 28: Transactivation data toward hPPAR*α* by **27a**, **27b** and **WY14643**.
(WY14643 is used as a standard of PPAR*α* full-agonist)

Based on encouraging *in vitro* and triglyceride reducing activity of the above two series, it was decided to replaced the oximino moiety of compound **V** and **27b** by methine moiety as in **33a-b**. Compound **33a** exhibited reduced activity of PPAR*α* (αEC_{50} = 1.0 µM, E_{max} = 155%) compared to compound **V** but did not show comparable *in vivo* efficacy**.** Compound **33b** also possessed weak PPAR*α* activity (αEC_{50} = 7.1 µM, E_{max} = 120%) and reduced serum triglyceride by 15% in *SAM* (**Table 16**). Interestingly, the methine moiety affect the selectivity profile of **33a** and **33b**. These compounds with methine linker are still flexible enough to adapt to PPAR*α* receptor. Based on the cumulative *in vitro* and triglyceride reducing activity of the above three series, the compound **27a** was selected as a lead compound for further biological evaluation.

Table 16. *In vitro* hPPAR transactivation and TG reducing activity of **33a-b**.

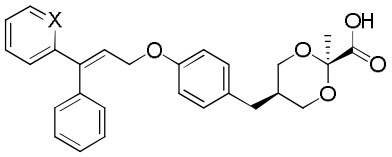

Compd	X	hPPAR Transactivation[a]					% Change in serum TG[e]
		α^b (10μM)	γ^b (0.2μM)	δ^b (10μM)	α^c % E_{max}	α^d EC_{50} (μM)	
33a	CH	16.15	IA	1.04	155	1.0	-25.3
33b	N *E* isomer	11.54	IA	IA	120	7.1	-15.0
V		16.28	IA	ND	181	0.14	-46.0
Fenofibrate		6.58	IA	1.51	90	10.8	-36.6[f]

[a]IA denotes inactive where compounds did not show any fold activation above basal level shown by vehicle (DMSO) and ND denotes not detemined. hPPAR denotes human PPAR.
[b]Activites are presented as fold induction of PPARα, γ and δ activation over basal level (DMSO).
[c]% *E*max (maximal efficacy) of all test compounds was compared to WY14643 (100% PPARα).
[d] EC_{50} is half maximal effective concentration.
[e]Values indicated are the mean of n= 6 and $p < 0.05$ vs vehicle control.
[f]Fenofibrate was administered orally at a dose of 300 mg/kg/day

To understand further and to draw correlation between weak *in vitro* potency and good *in vivo* efficacy of compound **27a**, its pharmacokinetic parameters were evaluated and the results are presented in **Table 17**. The compound **27a** showed rapid T*max*, good Cmax and AUC along with rapid half-life, when administerd orally to fasted male *Wistar* rat at a dose of 30 mg/kg/day. Compared to **V**, compound **27a** showed 6-fold higher Cmax, 5-fold higher AUC and equal half-life. These results clearly established the compound **27a** as a highly efficacious and bioavailable in animal model with weak *in vitro* potency.

Table 17. Mean pharmacokinetic parameters of **27a** in fasted male *Wistar* rat.

Compd.	Route	dose (mg/kg)	T_{max} (h)	C_{max} (μg/mL)	$T_{1/2}$ (h)	AUC(0-∞) (h.μg/mL)
27a	Oral	30	1.0 ± 0.0	15.96 ± 1.0	3.52 ± 0.3	55.08± 1.9
V	Oral	30	1.4 ± 0.6	2.61 ± 1.0	3.83 ± 0.4	11.27± 3.0

[a]Values indicate mean ± SD for n=6

In view of unique *in vitro* profile and favorable pharmacokinetic parameters, we evaluated compound **27a** for *anti*-hyperlipidemic and *anti*-hyperglycemic potential in *db/db* mice (dose, 3.0 mg/kg/day for 7 days). The compound **27a** demonstrated excellent triglyceride (TG) and plasma glucose lowering activities in *db/db* mice (**Table 18**).

Table 18. *In vivo* efficacy of the compound **27a** in *db/db* mice[a].

Compounds	*db/db* mice[a]		
	Dose (mg/kg/day)	% Change Vs Control	
		Serum TG	Serum Glucose
27a	3	-48.3	-28.0
Fenofibrate	300	-36.1	-35.5

[a] Values indicated are the mean of n= 6 and $p < 0.05$ vs vehicle control.

Compound **27a** was further evaluated in *Zucker fa/fa* rat, a model that develops massive obesity with hyperglycemia and hypertriglyceridemia. Compound **27a** was administered orally (0.3, 1, 3 and 10 mg/kg/day dose), for 14 days, maximum reduction of TG (61%) and total cholesterol (TC) (27%) was observed at 3.0 mg/kg/day dose (**Table 19**).

Table 19. *Anti*-hyperlipdemic and *anti*-hyperglycemic activity of **27a** in male *Zucker fa/fa* rat[a]

Dose (mg/kg/day)	% Change			
	TG	TC	Fed glucose	Fasted insulin
0.3	-15.7	8.2	ND	ND
1	-46.0	13.0	ND	ND
3	-61.0	-26.5	-17.8	-50.7
10	-59.7	-27.7	ND	ND

[a] Values indicated are the mean of n= 6 and $p < 0.05$ vs vehicle control. ND denotes not detemined

Next it was sought to demonstrate changes in LDL-C, HDL-C, serum TG and total cholesterol derived from PPAR mediated effects of **27a,** using high fat

and high cholesterol fed (HF-HC) hamsters, Wang et.al reported that high HF-HC hamster is a unique animal model to evaluate the effects of PPAR*α* selective agonist on dyslipidemia[245] Therefore HF-HC hamsters were treated with compound **27a** orally (3 mg/kg/day dose), for 14 days and the pharmacological effects (LDL-C, HDL-C, serum TG and total cholesterol (TC)) were measured at the end of the study (**Table 20**). The compound **27a** exhibited excellent reduction of serum TG, TC and LDL-C.

Table 20. *Anti*-hyperlipidemic activity of compound **27a** in HF-HC hamsters [a].

Compd	Dose (mg/kg/day)	% Change			
		TG	TC	LDL-C	HDL-C
27a	3	-77	-33	-46	-16
Fenofibrate	100	-44	-38	ND	ND

[a] Values indicated are the mean of n= 6 and $p < 0.05$ vs vehicle control. ND = not detected.

3.2.3 Molecular docking study

To understand the target selectivity profile of *Z* (**27a**) and *E* (**27b**) isomers, both compounds were docked into ligand binding domains of PPAR*α* and PPAR*γ*. The complex X-ray crystal structure of the ligand binding domain of PPAR*α* with GW409544 (1K71.pdb) and PPAR*γ* with Rosigliazone (2PRG.pdb) were obtained from RCSB protein data bank. Extensive literature survey on the structural aspects of the PPARs[31,240,246,247] suggested that interactions of the ligand with Tyr314, Tyr464, and Ser280 to be important for the activation of PPAR*α* and interactions of ligand with Ser289, His323, Tyr473 and His449 are important for PPAR*γ*.

The *Z* (**27a**) isomer adopted a conformation that allows the carboxylic group to form hydrogen bonds with Tyr464, Tyr314 and Ser280 in PPAR*α* (**Figure 29**). Quite expectedly the same isomer does not show any hydrogen bonding interactions with the key amino acids in PPAR*γ*. The *E* isomer (**27b**), when docked into PPAR*α* binding pocket, adopted a conformation that allows carboxylic acid group to form H-bond interactions with Tyr464 and Ser280 missing out Tyr314. While in PPAR*γ* binding pocket, *E* isomer (**27b**) although has

the standard binding mode but does not show up hydrogen-bonds that are required for selectivity. This docking study prompted to conclude that the *Z* isomer (**27a**) has more selectivity towards PPAR*α* compared to the *E* isomer (**27b**). Absence of these critical interactions with the protein might provide the structural basis for the much weaker transactivation activity of **27b** towards PPARα and PPARγ. In the light of these docking calculations it can be inferred that **27b** has weak selectivity and potency towards PPARα and PPARγ.

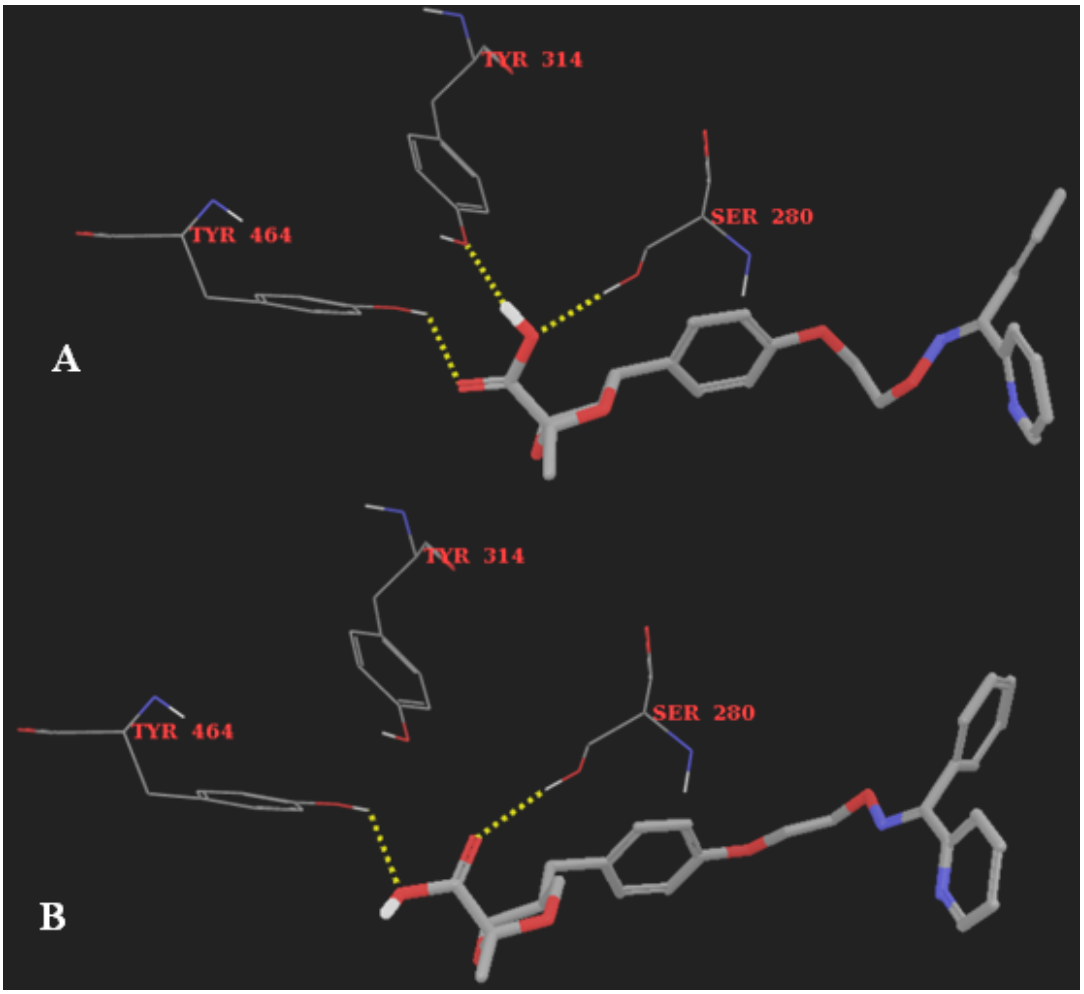

Figure 29: A. Molecular docking of **27a (*Z* isomer)** and **B**. **27b (*E* isomer)** into PPARα binding pockets: H-bond interactions with amino acids are shown in dashed lines.

3.3 Design and synthesis of PPARα/γ dual agonists

The research was focused on PPARα/γ dual agonists in order to combine the fuel storing and insulin sensitizing effect of PPARγ with lipid modulating effect of PPARα. Now the goal was to identifying potent and balanced PPARα/γ dual agonists applicable as tailored therapy for type-2 diabetes and associated co-morbidities.

3.3.1 Replacement of phenylene with naphthalene as a central aromatic spacer.

To synthesize compounds **46**, **51**, **54**, **57**, **66a**, **66b, 70** and **73** (**Figure 30**) 1,3-dioxane-*r*-2-carboxylic acid, Glycine, oximino acid and *α*-alkoxy-substiuted propanoic acid were treated as a head groups, which are binding motifs for the AF2-helix interface and which occur in clinically advanced PPARα/γ dual agonists such as **XI**[225], **Muraglitazar**[158], **Imiglitazar**[232] and **Tesaglitazar**[233] respectively.

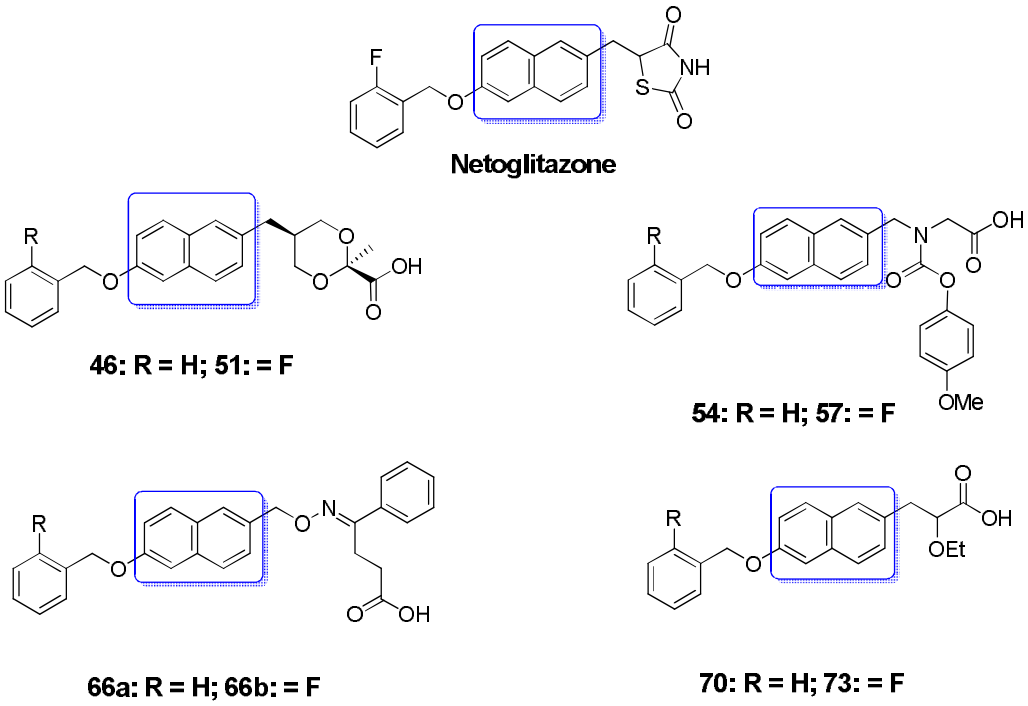

Figure 30: Chemical structure of Netoglitazone and PPAR coagonists.

For the cyclic tail, it was focused on the benzyloxy moiety and regarding aromatic center, it was decided to explore the potential of bicylic core specifically naphthalene present in Netoglitazone (**Figure 30**).

3.3.1.1 Chemistry

Synthesis of compounds **38** was undertaken as follows. Bromonation of β naphthol **34** in presence of bromine and tin in acetic acid under reflux condition lead to the formation of compound **35**.[248] Benzyation of **35** with benzyl bromide (**36**) in the presence of potassium carbonate, as a base, in dimethylformamide, resulted to compound **37**. Formyaltion of **37** was accomplished by lithium halogen exchange, followed by quenching with dimethylformamide, to afford the aldehyde (**38)**, with unexpected product **39**, with butyl chain at the benzylic position (**Scheme 7**).[249]

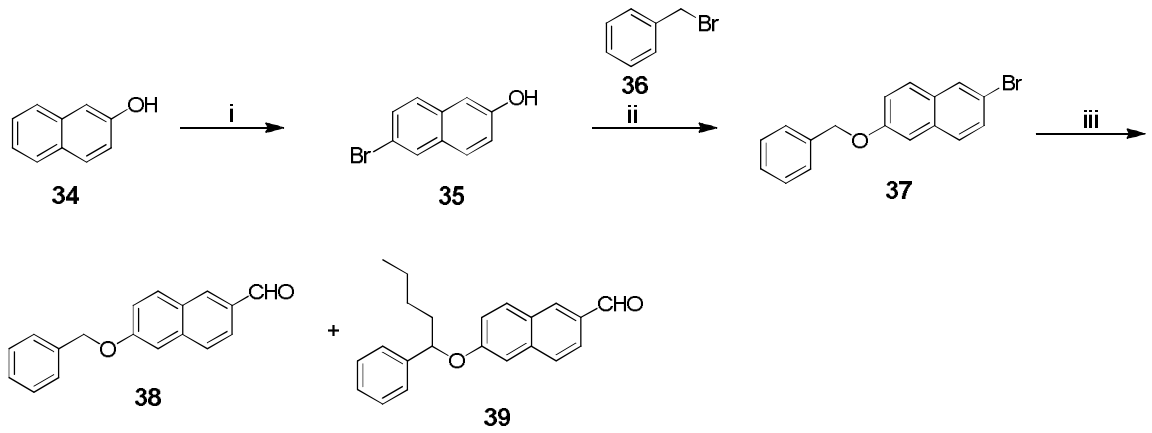

Scheme 7. Reagents and conditions: i) Acetic acid, Bromine, Tin, reflux, 3 hrs, 90%; ii) K_2CO_3, Benzyl bromide, DMF, 80 °C, 1 hr, 95%; iii) n-BuLi, DMF, THF, 25 °C, 3.0 hrs, 13%.

For the preparation of the compounds **46** and **51** (**Figure 30**), the alcohol **40** was obtained by reduction of aldehyde **38**, using sodium borohydride. The alcohol on treated with thionyl chloride in chloroform yielded **41**, which on reaction with the enolate of diethylmalonate gave **42** which was reduced to diol **43** using $LiAlH_4$. Transformation of **43** to dioxane **44** (*cis* + *trans*) was achieved by the treatment of **43** with methyl pyruvate and boron trifluoride diethyl ether

complex. The attempts to separate the *cis* and *trans* isomers of **44** by column chromatography were unsuccessful (**Scheme 8**).

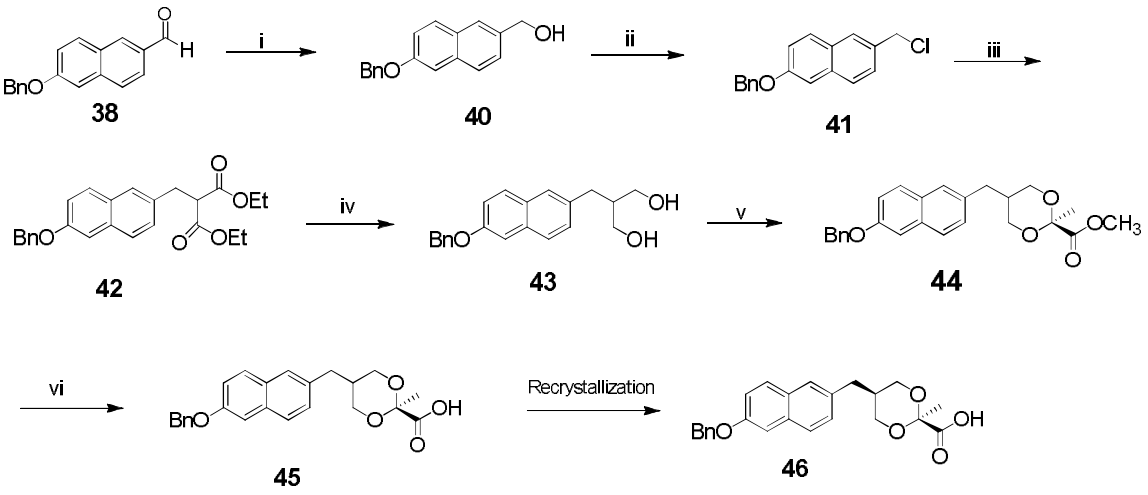

Scheme 8. Reagents and conditions: i) $NaBH_4$, THF:MeOH, 30 °C, 1.0 hrs, 98%; ii) Thionyl chloride, chloroform, 30 °C, 5.0 hrs, 93%; iii) Diethyl malonate, NaH (60%), THF, 48 °C, 14 hrs, 90%; iv) $LiAlH_4$, THF, 25 °C, 6 hrs, 70%; v) Methyl pyruvate, BF_3:Et_2O, CH_3CN, 25 °C, 1 hr, 71%; vi) $LiOH.H_2O$, THF:CH_3OH:H_2O, 25 °C, 4 hrs, 46%.

Debenzylation of the mixture of isomers **44**, under hydrogenation conditions (using Pd/C and ammonium formate) yielded the compound **47**. Compound **49** was obtained by treating **47** with o-fluoro benzyl bromide **48**, in the presence of potassium carbonate and dimethyl formamide (**Scheme 9**). The desired esters **44** and **49** were hydrolyzed by using lithium hydroxide, to give the carboxylic acids, **45** and **50** respectively, containing mixture of *cis* and *trans* isomers. Separation of *cis* isomer was carried out by repeated crystallization from a mixture of 1:2 ethyl acetate and hexane, so that c*is* isomers **46** and **51** were obtained quantitatively with minor quantity of *trans* isomer. The stereochemistry of compounds **46** and **51** is established as *cis* isomers, based on ^{1}H NMR data, wherein the chemical shift data of **46** and **51** were found to be in accordance with the similar compound reported earlier.[225, 250]

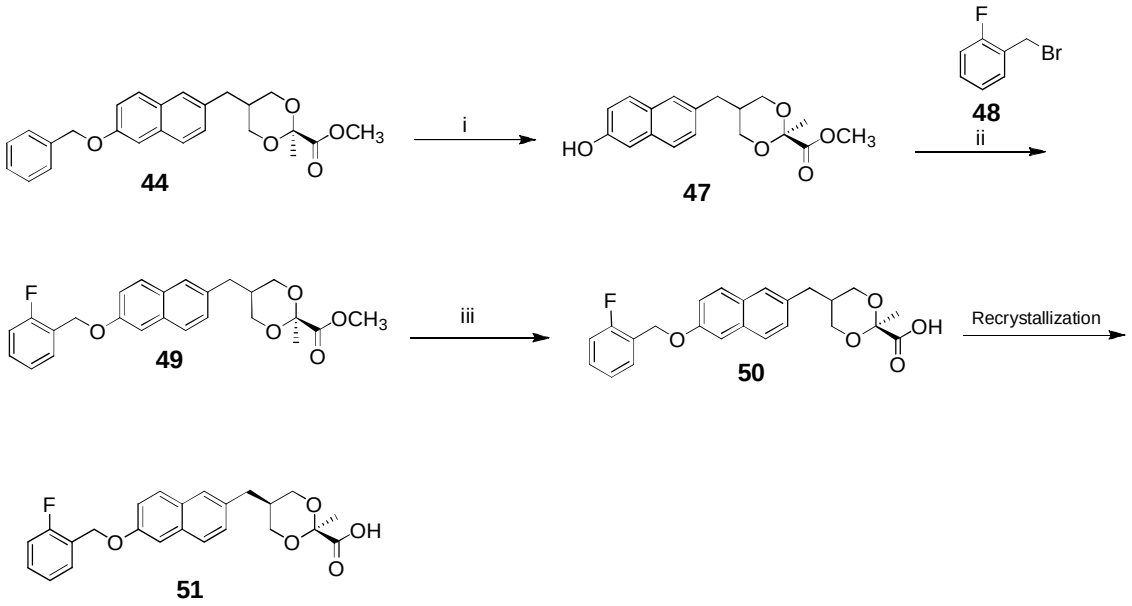

Scheme 9. Reagents and conditions: i) Pd/C, $HCOONH_4$, CH_3OH, reflux, 1 hr, 71%; ii) K_2CO_3, DMF, 80 °C, 18 hrs, 59%; iii) $LiOH.H_2O$, $THF:CH_3OH:H_2O$, 25 °C, 18 hrs, 38%.

Synthesis of the compounds **54** and **57**, was undertaken from the aldehyde **38** which was reacted with glycine ethyl ester hydrochloride, in triethyl amine and methanol mixture, under standard reductive amination conditions using sodium triacetoxyborohydride[251] provided secondary amine **52**. Reaction of amine **52** with 4-methoxyphenyl chloroformate, in dichloromethane gave N-acylated ethyl ester **53**, which on aqueous basic hydrolysis afforded **54** (**Scheme 10**).

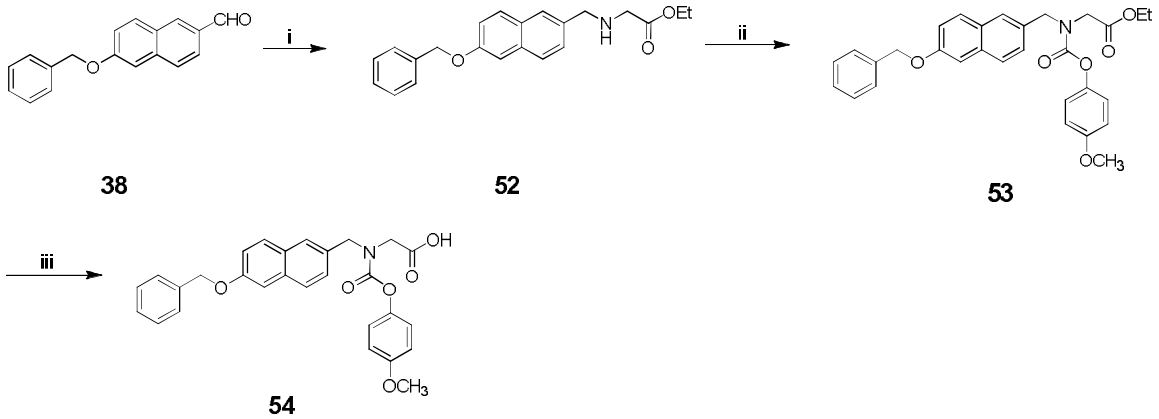

Scheme 10. Reagents and conditions: i) Glycine ethyl ester hydrochloride, Et_3N, sodium triacetoxyborohydride, MeOH, 30 °C, 15 hrs, 25%; ii) 4-Methoxyphenyl chloroformate, CH_2Cl_2, 25 °C, 2 hrs, 69.37%; iii) $LiOH.H_2O$, THF, MeOH, H_2O, 30 °C, 3 hrs, 25%.

Debenzylation of **53** in the presence of palladium on carbon (Pd/C) and ammonium formate, in methanol yielded **55**. Benzylation of **55** with the *o*-fluoro benzyl bromide (**48**) in presence of cesium carbonate gave the ester **56**. Finally compound **56** was hydrolysed with aqeous basic hydrolysed to yield **57** (**Scheme 11**).

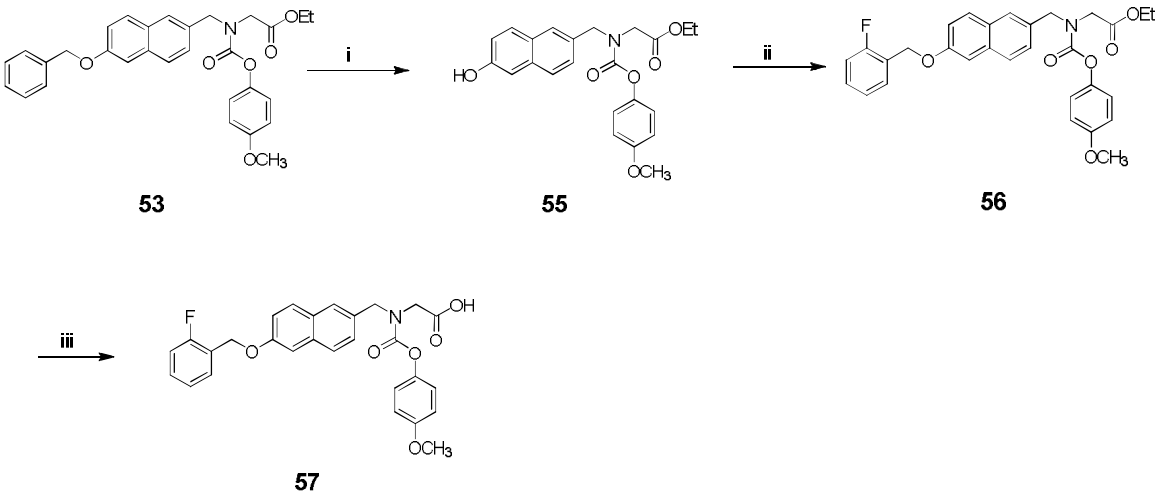

53 **55** **56** **57**

Scheme 11. Reagents and conditions: i) Pd/C, Ammonium formate, MeOH, reflux, 2 hrs, 76%; ii) *o*-Fluoro benzyl bromide (**48**), Cs_2CO_3, DMF, 80 °C, 3 hrs, 83%; iii) $LiOH.H_2O$, THF: MeOH: H_2O, 30 °C, 3 hrs, 67%.

Synthesis of intermediate **60** is depicted in **Scheme 12**. Intermediate **58** prepared by Friedel-craft acylation of benzene with succinic anhydride was esterified using thionyl chloride in methanol to giving the methyl ester (**59**). Treatment of **59** with hydroxylamine hydrochloride and sodium acetate in ethanol gave oxime derivative, as a mixture of *E* and *Z* isomers and the *E* isomer (**60**) was isolated as a major product on column chromatography. The ^1H NMR chemical shifts were identical with the reported values.[232]

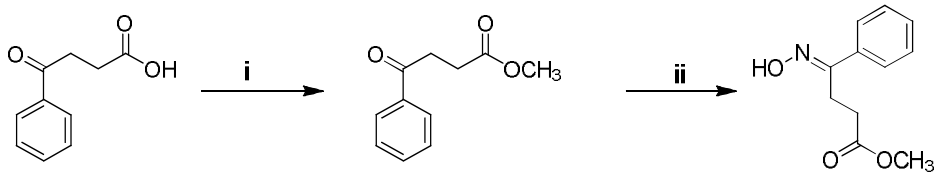

58 **59** **60**

Scheme 12. Reagents and conditions: i) Thionyl chloride, methanol, reflux, 4 hrs, 96.4%; ii) Hydroxylammonium chloride, sodium acetate, ethanol, reflux, 5 hrs, 76%.

Synthesis of compounds (**66a-b**) started with the benzylation of 6-Bromo-β-naphthol, with benzyl bromide (**36)** or 2-fluorobenzyl bromide, (**48**) in presence potassium carbonate in dimethylformamide giving **37** and **61** respectively. Formylation of **37** and **61**, with dimethylformamide in dry tetrahydrofuran yielded the desired aldehydes **38** and **62** respectively. Aldehydes on reduction with sodium borohydride yielded **40** and **63** which were treated with thionyl chloride, in chloroform to give the chlorides **41** and **64**. Coupling reaction between **41** and **64** with oxime (**60**) in the presence of cesium carbonate and dimethyl formamide gave esters **65a** and **65b** which upon hydrolysis under aqueous basic condition gives the acids **66a-b** (**Scheme 13**).

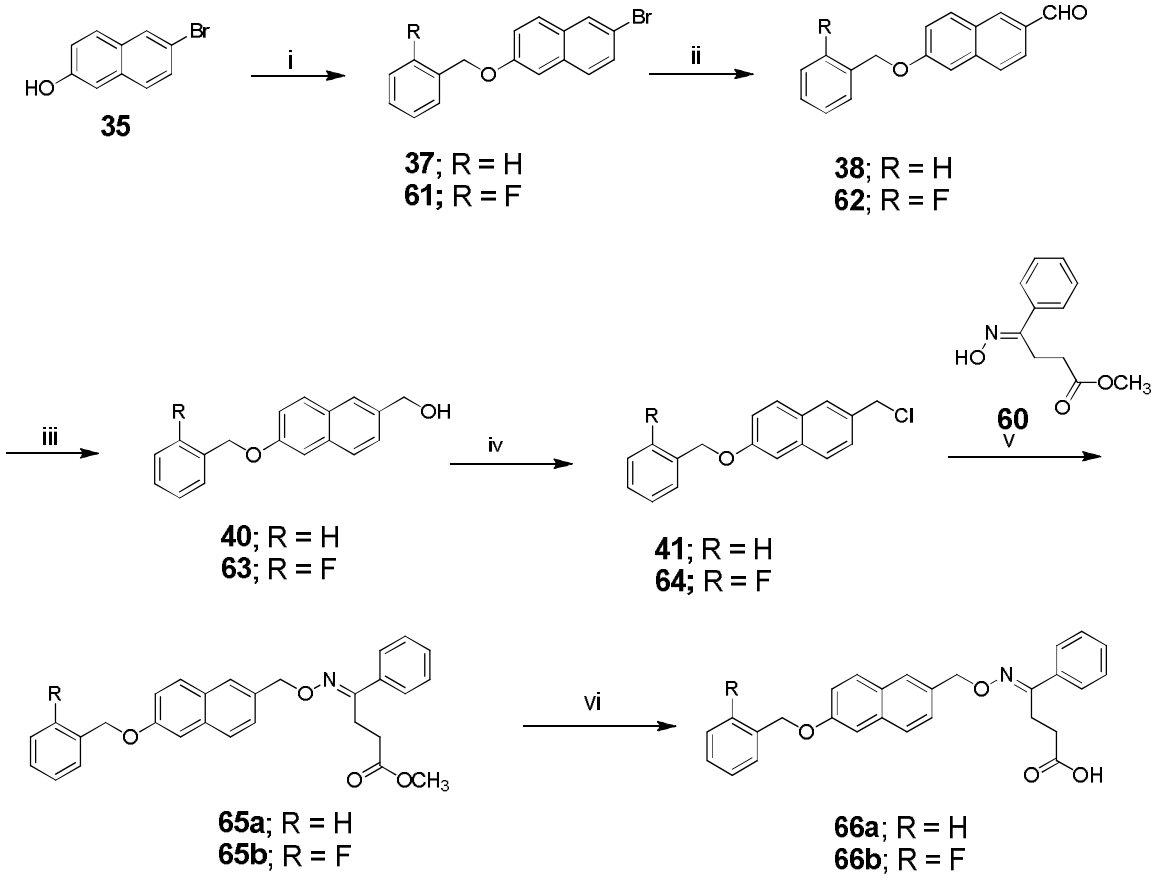

Scheme 13. Reagent & conditions: i) **36** or **48**, K_2CO_3, DMF, 80 °C, 1 hr, 74 - 95%; ii) *n*–BuLi, Dimethylformamide, THF, 25 °C, 3 hrs, 13 - 35%; iii) $NaBH_4$, THF:MeOH, 30 °C, 1.0 hrs, 98%; iv) Thionyl chloride, chloroform, 30 °C, 4 - 5 hrs, 70-93%; v) Cesium carbonate, DMF, 30 °C, 12-15 hrs, 47 - 70%; vi) $LiOH.H_2O$, THF: CH_3OH :H_2O, 30 °C, 2.0 hrs, 70%.

For the synthesis of compound **70**, Darzen's condensations of **38** with ethyl chloroacetate in the presence of potassium carbonate using tetra-*n*-butylammonium bromide (TBAB) as a phase transfer catalyst, in dimethyl formamide yielded α, β epoxy ester (**67**). Catalytic hydrogenation of **67** gave racemic secondary alcohol (**68**). Alkylation of the alcohol with diethyl sulfate using potassium hydroxide yielded *α*-ethoxy ester (**69**). Hydrolysis of ester (**69**), using lithium hydroxide yielded the acid **70** (**Scheme 14**).

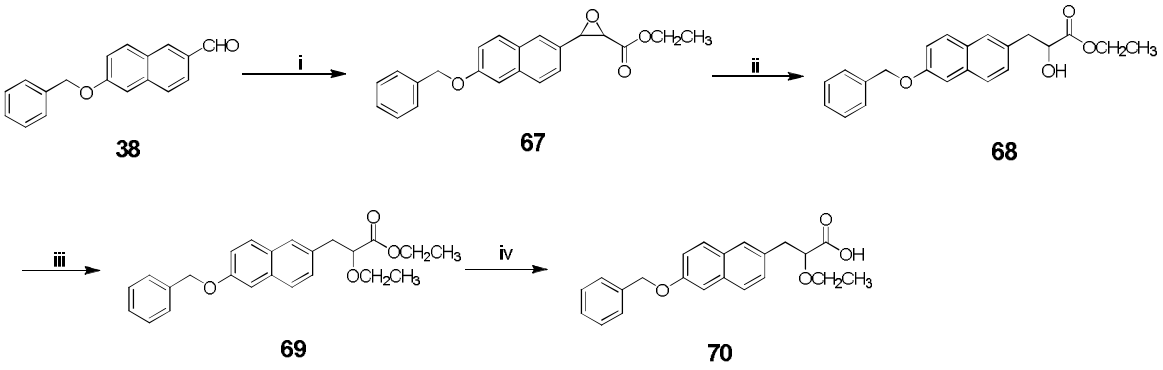

Scheme 14. Regents and conditions: i) K_2CO_3, Ethyl chloroacetate, tetra butyl ammonium bromide, DMF, 30 °C, 25 hrs, 82%; ii) H_2, Pd/C, 1,4 dioxane, 30 °C, 5-10 psi, 15 hrs, 48%; iii) KOH, DMSO, diethyl sulfate, 30 °C, 5 hrs, 99%; iv) $LiOH.H_2O$, THF: CH_3OH: H_2O, 25 °C, 18 hrs, 50%.

Catalytic hydrogenation of **69**, in the presence of Pd/C and ammonium formate, in methanol under reflux condition yielded phenol (**71**). Coupling of o-Fluoro benzyl bromide (**48**) and **71**, with cesium carbonate in dimethylformamide to yield ester (**72**), which upon basic hydrolysis gave **73** (**Scheme 15**).

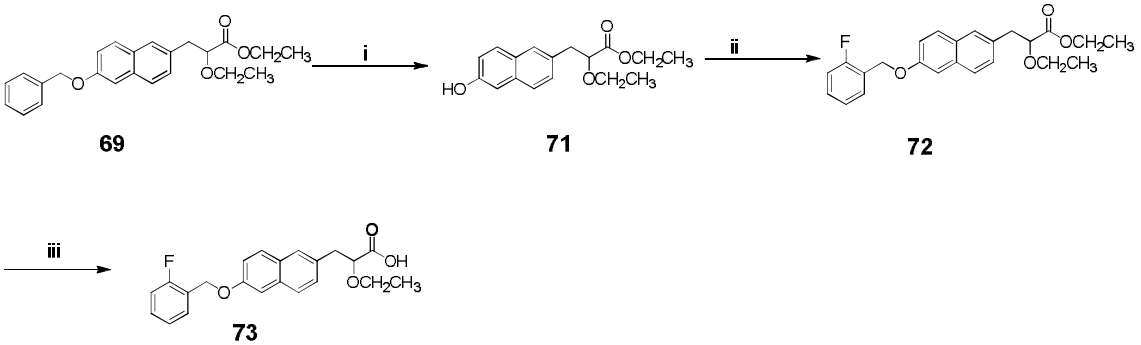

Scheme 15. Regents and conditions: i) $HCOONH_4$, Pd/C (10%), CH_3OH, reflux, 5 hrs, 43% ii) *o*-Fluoro benzyl bromide (**48**), Cesium carbonate, DMF, 30 °C, 18 hrs, 58%; iii) $LiOH.H_2O$, THF: CH_3OH: H_2O, 25 °C, 18 hrs, 54%.

3.3.1.2 Biology

In order to assess the potency and subtypes selectivity, all the test compounds synthesized (**46**, **51**, **54**, **57**, **66a**, **66b, 70** and **73**) were screened *in vitro* for hPPARα, γ and δ agonistic activity (PPAR transfected in HepG2 cells) according to the procedure described earlier. The **WY-14643** (PPARα), **GW-501516** (PPAR*δ*) and **Rosiglitazone** (PPARγ) were used as standard compounds and the *in vitro* activity results (fold inductions Vs vehicle control (DMSO; 1% solution)) and *in vivo* TG lowering activity are summarized in **Table 21**. As described earlier, our goal was to develop balanced PPARα/γ dual agonist. In this attempt, we intended to replace the phenylene group with naphthalene as a central aromatic spacer with benzyloxy group as lipophilc tail of **I**, **Imiglitazar**, **Muraglitazar** and **Teasaglitazar** (potent PPARα/γ dual activators). Compounds **46** and **51** with 1,3-dioxane-*r*-2-carboxylic acid head exhibited hPPARα.selectivity and compound **51** reduced serum triglyceride by 21% in *Swiss albino mice* (*SAM*). Compounds **54** and **57** with glycine acidic head were found to be inactive in PPAR*α* and possessed weak agonistic activity in PPARγ and PPAR*δ*. While compounds with oximino acid acidic head (**66a-b**) exhibted good selectivity towards PPAR*δ* with weak PPARγ activity and found to be inactive in PPARα. Compound **66b** showed superior activity towards PPAR*δ* compared to **66a.** Compounds **70** with *α*-alkoxy-substiuted propionic acid head group exhibit balanced and potent activity in PPARα (E_{max} = 154% compared to WY14643 (defined as 100%)) and PPARγ (E_{max} = 142% compared to Rosiglitazone (defined as 100%)). Compound **70** and **73** showed 60.2% and 57% reduction of TG in *SAM,* respectively.

Table 21. *In vitro* hPPAR transactivation and TG reducing activity of compounds **46**, **51**, **54**, **57**, **66a-b**, **70** & **73**.

Compound	hPPAR Transactivation[a,b]			% Change in serum TG[c]
	α (10μM)	γ (0.2μM)	δ (10μM)	
46	5.89	1.19	1.37	ND
51	5.27	1.79	1.25	-21.0
54	IA	1.82	1.21	ND
57	IA	1.76	1.02	-9.1
66a	IA	1.35	1.65	ND
66b	IA	1.78	2.85	ND
70	10.05	12.47	1.26	-60.2
73	ND	ND	ND	-57.2
Tesaglitazar				-67.1
vehicle	1.0	1.0	1.0	
WY-14643	6.51	ND	ND	
Rosiglitazone	IA	8.75	IA	
GW-501516	ND	ND	4.77	

[a]IA denotes inactive where compounds did not show any fold activation above basal level shown by vechile and ND denotes not detemined. hPPAR denotes human PPAR.
[b]Activites are presented as fold induction of PPARα, γ and δ activation over basal level (DMSO).
[C]Values indicated are the mean of n= 6 and $p < 0.05$ vs vehicle control.

Compound **70** which exhibited balanced hPPARα : γ ratio was selected for further profiling. **Table 22** summarizes the results of compound **70**. After adminstrating compound **70** for 7 days to *db/db* mice, at a dose of 3 mg/kg/day. Compound **70** exhibited comparable *in vivo* activity with Tesaglitazar.

Table 22. *Anti*-Hyperglycemic and *anti*-hyperlipidemic activities of **70** in *db/db* mice[a]

Compound	Dose (mg/kg/day)	% Change		% improvement in BC AUC Glucose Vs control
		TG	PG	
70	3	-62	-73	58.3
Tesaglitazar	3	-60	-54	61

[a] Values indicated are the mean of n= 6 and $p < 0.05$ vs vehicle control.

Compound **70** was further profiled in high fat, high chloesterol (HF-HC) fed hamster for antihyperlipidemic activity (**Table 23**). Compound **70** illustrates the similar effect, when directly compared to Tesaglitazar at a dose of 3 mg/kg/day.

Table 23. *Anti*-hyperlipidemic activities of compounds **70** in HF-HC hamsters[a]

Compounds	Dose (mg/kg/day)	% Change Vs Control		
		LDL-C	HDL-C	TC
70	3	-48	-28	-31
Tesaglitazar	3	-46	-20	-40

[a] Values indicated are the mean of n= 6 and $p < 0.05$ vs vehicle control.

3.3.1.3 Molecular docking Study

The molecular docking analysis of compound **70** and netoglitazone was carried out to infer its selectivity profile and critical interactions with the active site of PPAR*α,* PPARγ and PPAR*δ* binding pockets, using Glide version 6.7. Briefly, the automated docking program implemented in the Schrodinger package. The geometry of docked compound (**70** and netoglitazone) was subsequently optimized using the LigPrep version 2.6. The complexed X-ray crystal structure of the ligand binding domain (LBD) of PPARα with GW409544 (1K7l.pdb) and PPARγ with Rosiglitazone (2PRG.pdb) and PPAR*δ* with D32 (3GZ9.pdb) were obtained from RCSB protein Data Bank. As depicted in **(Figure 31)**, when **70** was docked into PPARα binding pocket, the most stable docking models of **70** adopted a conformation that allows the carboxylic group to form hydrogen bonds with Tyr314, Tyr464, and Ser280, which have been reported to be essential interaction for PPARα selective compounds. When **70** was docked into PPARγ binding pocket the most stable docking model of compound **70** adopted a conformation that allows the carboxylic group to form hydrogen bonds with Ser289, His323, His449 and Tyr473. When compound **70** was docked into PPAR*δ* binding pocket the most stable docking model of **70** adopted a conformation that allows the carboxylic group to form hydrogen bonds only with His 449 and the literature precedence suggests that interaction of the ligand with

Thr289, His323, Tyr473 and His449 are important for PPAR*δ* affinity, as this H-bonding network could stabilize the AF-2 helix in a conformation, which favors the binding of co-activators to PPAR*δ*. Thus favorable *in-silico* interaction of compound **70** with PPAR*α* binding pocket and with PPARγ binding pocket might correlate its *in vitro* selectivity profile toward PPAR*α* and PPARγ.

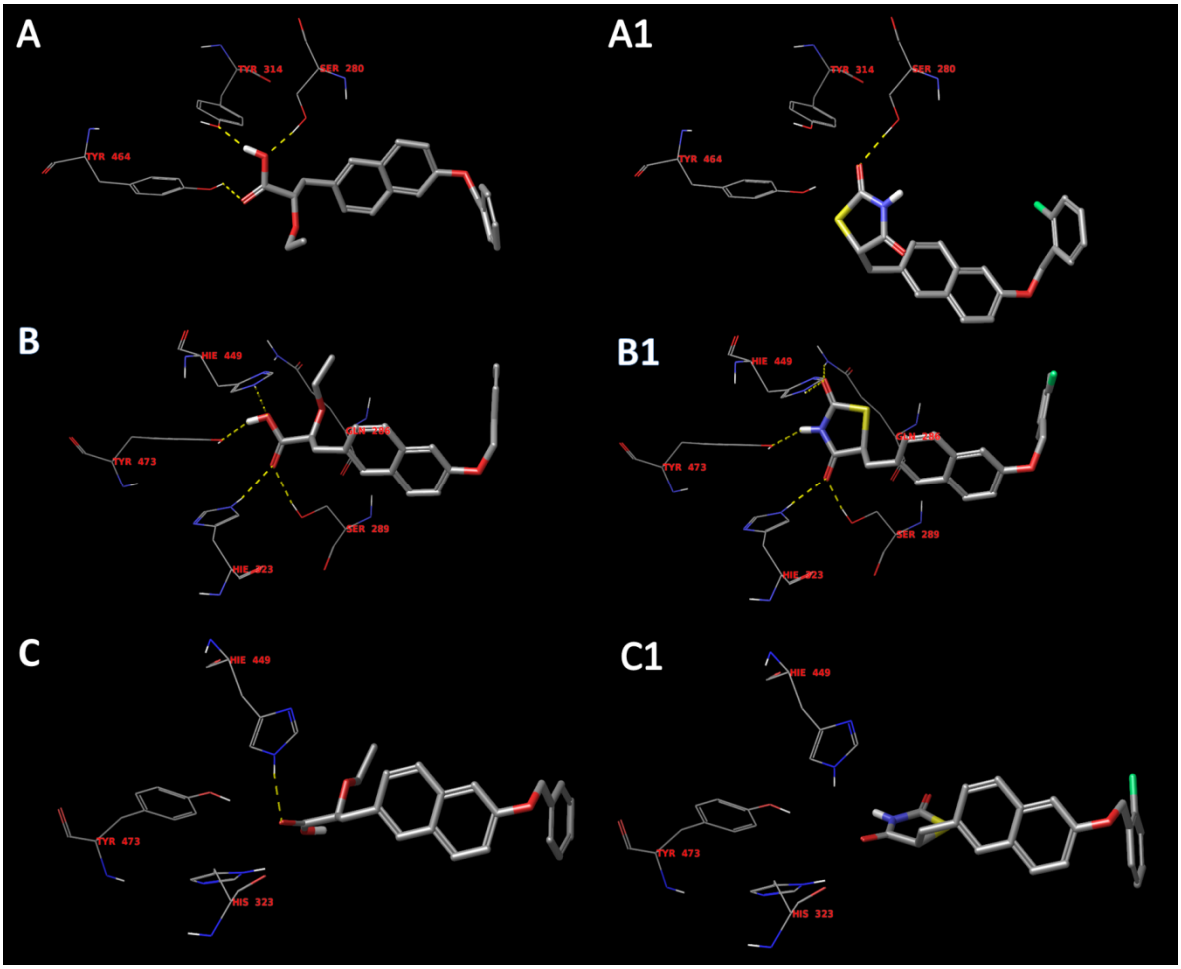

Figure 31: Molecular docking of **70** into PPARα (A) and γ (B) and *δ* (C) binding pockets and molecular docking of Netoglitazone into PPARα (A1) and γ (B2) and *δ* (C1) binding pockets: H-bond interactions with amino acids are shown in dashed lines.